Cardiovascular drug delivery with ultrasound and microbubbles ☆

Evan Unger [a,*], Thomas Porter [b], Jonathan Lindner [c], Paul Grayburn [d]

[a] Depts. of Radiology and Biomedical Engineering, The University of Arizona Health Sciences Center, Tucson, AZ, USA
[b] Dept. of Cardiology, University of Nebraska Medical Center, Omaha, NE, USA
[c] Division of Cardiovascular Medicine, Oregon Health & Science University, Portland, OR, USA
[d] Baylor Heart and Vascular Center, Dallas, TX, USA

ARTICLE INFO

ABSTRACT

Microbubbles lower the threshold for cavitation of ultrasound and have multiple potential therapeutic applications in the cardiovascular system. One of the first therapeutic applications to enter into clinical trials has been microbubble-enhanced sonothrombolysis. Trials were conducted in acute ischemic stroke and clinical trials are currently underway for sonothrombolysis in treatment of acute myocardial infarction. Microbubbles can be targeted to epitopes expressed on endothelial cells and thrombi by incorporating targeting ligands onto the surface of the microbubbles. Targeted microbubbles have applications as molecular imaging contrast agents and also for drug and gene delivery. A number of groups have shown that ultrasound with microbubbles can be used for gene delivery yielding robust gene expression in the target tissue. Work has progressed to primate studies showing delivery of therapeutic genes to generate islet cells in the pancreas to potentially cure diabetes. Microbubbles also hold potential as oxygen therapeutics and have shown promising results as a neuroprotectant in an ischemic stroke model. Regulatory considerations impact the successful clinical development of therapeutic applications of microbubbles with ultrasound. This paper briefly reviews the field and suggests avenues for further development.

© 2014 Elsevier B.V. All rights reserved.

Contents

---

1. Introduction

Microbubbles are FDA approved in the US with indications for echocardiography [1]. Work is underway to gain approval in the US for radiology indications as well, but at the time of preparation of this review, microbubbles are not yet approved for radiology ultrasound imaging in the US [2]. In Europe and Canada, however, microbubbles are approved for both echocardiography and radiology indications [3,4]. Microbubbles present an acoustic impedance mismatch between biological fluids and tissues, are highly compressible and are highly reflective to ultrasound; hence microbubbles are highly effective as contrast agents for diagnostic ultrasound [5–7]. The purpose of this review is to present the potential therapeutic applications of microbubbles within the cardiovascular field and the diagnostic applications of approved microbubble-based contrast agents will not be covered by this review. As targeted microbubble agents might also be used for therapeutic as well as diagnostic molecular imaging applications, however, this review will also cover targeted microbubbles for cardiovascular applications [8,9]. In addition to their role as therapeutic agents with ultrasound, microbubbles can also be used for oxygen delivery and this review will present some of these potential applications for treating cardiovascular disease as well [10,11].

The microbubbles that are currently approved or in clinical trials all contain fluorinated gases. Coatings of lipid, protein or polymer shell stabilize them. There are currently two FDA approved microbubble-based agents in the US, Definity® and Optison®. A layer of phospholipid coats Definity microbubbles and Optison microbubbles are coated by a layer of denatured human serum albumin. The coating material envelops the microbubbles and helps to control microbubble size as well as to maintain microbubble stability. Another agent, EchoGen®, was composed of dodecafluoropentane emulsion (DDFPe) nanodroplets stabilized by a fluorosurfactant, PEG-Telomer-B [12,13]. The boiling point of DDFP is about 28 °C. Because of surface tension effects, DDFPe did not truly form microbubbles following IV injection, and had to be activated (e.g. hypobaric activation by pulling back on the syringe to create negative pressure and thereby create microbubbles for use as an ultrasound contrast agent [14]). EchoGen was approved by the European Medicines Agency (EMEA) and approvable by the US FDA but never launched [15]. The currently approved agents in the US are based upon perfluoropropane (boiling point about −34 °C). Sonazoid® which is approved in Japan is based upon perfluorobutane (boiling point about −1.4 °C) and BR-14 and BR-55 are also based upon perfluorobutane [16–18]. Microbubbles either approved by the FDA, the European Medicines Agency, or currently in clinical trials are described in Table 1.

Fluorinated gases are used in the above agents because of the low solubility of these materials in aqueous media. The fluorinated gases are less soluble than air, nitrogen or oxygen. The less soluble gases dissolve more slowly affording production of longer-lived microbubbles useful for ultrasound imaging and also potentially for cardiovascular drug delivery [25]. In general, the higher the molecular weight of the gas, the lower the solubility. Of the gases shown in Table 1 perfluoropentane is the least soluble, perfluorobutane the next least soluble, sulfur hexafluoride the most soluble and perfluoropropane intermediate. As shown in Table 1, two of the approved microbubble products have phospholipid coatings and one of the microbubble products is stabilized by denatured albumin protein. One of the products, Sonozoid, is coated with phosphatidylserine (PS), an anionic form of phospholipid [21]. PS is accumulated by macrophages and this agent is used for liver imaging [26]. Two products are in clinical trials in Europe, both based upon phospholipid-coated perfluorobutane microbubbles [17,18]. BR-55 also contains a lipopeptide targeted to the receptor for vascular growth factor (VEGFR2) [18].

The mean size of Definity (perflutren) microbubbles is around 1 μm but particles range in size from several microns to submicron. Definity is prepared by agitation of a sealed vial of phospholipids and a headspace of perfluoropropane gas. The mean size of the microbubbles in one study was about 3–4 μm immediately after agitation and preparation and about 2 μm more than 24 h later [27]. In another study of Definity, the mean size of the microbubbles changed over a period of 3 h from about 3 μm to 0.98 μm with increasing decanting time [28]. The mean size of Optison is probably larger, with a mean size listed on the prescribing information of 3–4 μm and 95% of particles <10 μm and few particles as large as 32 μm [20]. The measured size of the microbubbles depends in part on the measurement system. Some systems such as quasi-elastic light scattering are more sensitive to sub-micron sized particles while other systems, e.g. optical particle sizing and light-obscuration systems, are more sensitive to particles larger than a micron. We show particle sizing for DDFPe (NuvOx Pharma, Tucson, AZ), identical to EchoGen described above, except that DDFPe contains a buffer helping to stabilize the formulation (EchoGen was unbuffered) (Fig. 1) [10]. Sizing of DDFPe with dynamic light scattering reveals a mean particle size of about 296 nm. Particles larger than 1 μm are essentially invisible to the dynamic light scattering system [29]. The light obscuration system (e.g. Accusizer) shown below, however, is sensitive to particles ranging from about 0.5 μm up to about 500 μm in size. For most microbubble preparations, which predominantly contain particles over 1 μm in size, the light obscuration kind of system is probably most appropriate. To characterize a formulation that contains a substantial population of submicron particles, e.g. Definity or EchoGen, both kinds of particle sizing systems are necessary to fully characterize the microbubble preparation [29,30]. Note that the largest particles, e.g. >10 μm in size are most apt to cause adverse bioeffects, and particle sizing is therefore an important measure to ensure product safety [31,32]. We have used the Accusizer to study DDFPe after hypobaric activation and mean particle size increases to about 2.2 μm (unpublished data).

1.1. Cavitation

Depending upon the acoustic intensity of the ultrasound used to insonate the microbubbles, the microbubbles may oscillate. The

Table 1
Microbubble contrast agents that are approved or currently in clinical trials.

Agent	Company	Coating	Gas	Place approved
Definity [19]	Lantheus	Phospholipid	Perfluoropropane	US and Canada
Optison [20]	GE Healthcare	Human serum albumin	Perfluoropropane	US
Sonazoid [21]	GE Healthcare	Phosphatidylserine	Perfluorobutane	Japan
Sonovue [22]	BRACCO	Phospholipid	Sulfur hexafluoride	Europe
BR-14 [17]	BRACCO	Phospholipid	Perfluorobutane	Clinical trials in Europe
BR-55 [18]	BRACCO	Phospholipid/lipo-peptide	Perfluorobutane	Clinical trials in Europe
EchoGen [12]	Sonus	PEG-Telomer-B	Dodecafluoropentane	EMEA*
Imagify [23]	Acusphere	Poly-lactic glycolic acid [24]	Perfluorobutane	MAA to EMEA**

* EchoGen was approved by the EMEA and approvable by the FDA. The corporate sponsor voluntarily withdrew the product from the EMEA. A reformulated version of DDFPe is currently under development by NuvOx Pharma, Tucson, AZ, as an oxygen therapeutic [10].

** The Market Authorization Application (MAA) was recently submitted by Acusphere to the EMEA for Imagify [24].
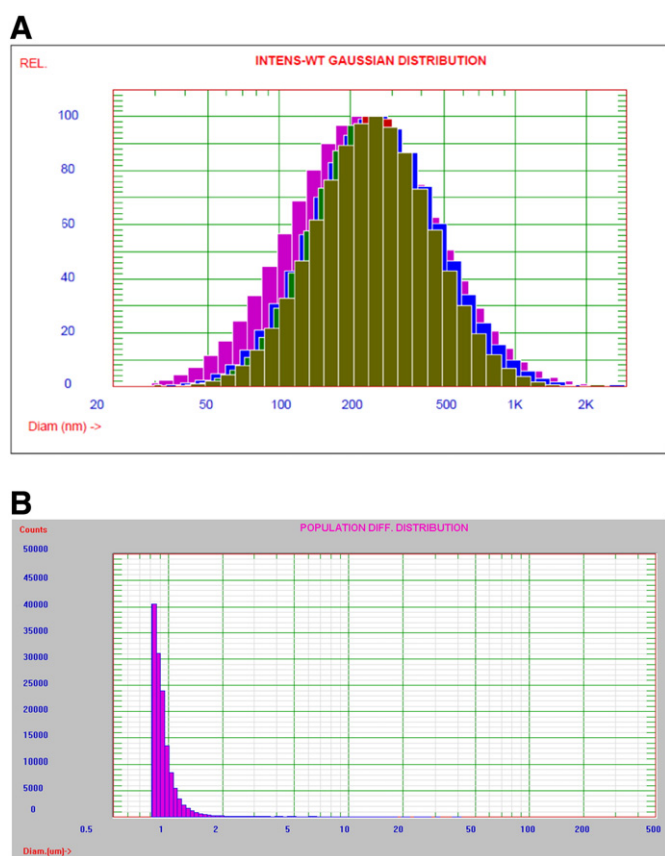
Fig. 1. A. Dynamic light scattering particle sizing of DDFPe. B. Optical particle sizing (light obscuration method) of DDFPe. Representation of larger particles of DDFPe, (shown in the left) calculated at 99.7% of the particle volume is less than 1400 nm PSS AccuSizer, Single-Particle Optical Sensing (SPOS). Note that the Accusizer is sensitive to particles ranging in size from 0.5 to 500 μm. The larger particles are not detectable by the Nycomps. USP 729 requires two different particle-sizing methods for parenteral emulsions [33].

Fig. 2. Cavitation of acoustically active liposphere. Streak image from ultra-high speed videomicroscopy with individual frame images shows resting droplet and effects from a single pulse of ultrasound energy above the inertial cavitation threshold. The particle expands, fragments, the fragments then expand again and collapse. Images courtesy of Kathy Ferrara, UC Davis and Paul Dayton, University of North Carolina.

oscillation may be repetitive and relatively stable in response to multiple pulses of ultrasound (stable cavitation) or may be violent wherein the microbubble is destroyed in response to a single pulse of ultrasound (inertial cavitation) [34,35]. An example of inertial cavitation is shown below in Fig. 2. In cavitation, the microbubbles compress during the peak positive pressure and expand in response to the negative rarefaction component of the ultrasonic wave. As stable cavitation occurs this creates a pulsing action that may create jets of fluid to increase permeability of drugs into clot or tissue [36]. Stronger cavitation will cause stronger acoustic jetting, fluid and tissue displacement as well as bioeffects and cell death. Both stable cavitation and inertial cavitation have therapeutic applications. By targeting ultrasound to a specific region, ultrasound targeted microbubble destruction (UTMD) can be exploited for therapeutic applications in the cardiovascular system.

1.2. Radiation force

In addition to cavitation, another mechanism that is important in cardiovascular drug delivery with ultrasound is radiation force (see Fig. 3). Ultrasound creates a pushing force and will push microbubbles away from the transducer face. The radiation force of ultrasound can be used to push microbubbles towards a target tissue. The particles might be concentrated in the target zone and then cavitation exploited for local drug delivery and therapy [37,38].
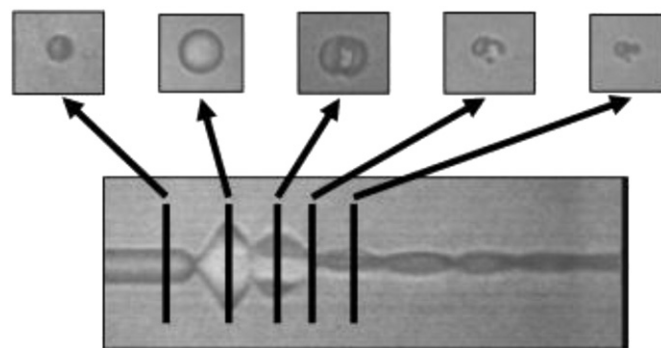
1.3. Microbubble designed for drug and gene deliveries

Microbubbles can be designed for drug and gene delivery applications. Fig. 4a and b depict two potential microbubble designs for gene delivery [39].

Fig. 4a and b depict two different kinds of phospholipid microbubbles for gene delivery. A cationic microbubble (left) contains cationic lipids in the membrane to form an association with anionic drug such as DNA. Fig. 4a depicts a cationic microbubble binding DNA which also contains lipid binding polyethyleneglycol (PEG). A targeting ligand (green triangle) may be affixed to the free end of the PEG molecules to bind to targets such as integrins on endothelial cells. Fig. 4b depicts a microbubble binding nanoparticles, e.g. condensed DNA in nanoparticles. PEG may be affixed to the nanoparticles or the lipids on the microbubble. Targeting ligands may also be incorporated onto the nanoparticles or the surface of the microbubble.

Microbubbles generally have low loading capacities for drugs. A film of oily material can be incorporated into lipid coated microbubbles to deliver hydrophobic drugs that are insoluble in the acqueous media and solube in the oil [40]. Microspheres can be used to load relatively high payloads of drug [41]. By filling the microspheres with gas and drug, the microspheres can still be acoustically responsive and subject to radiation force and cavitation [42].

DNA and RNA are polyanions and can be coupled to cationic microbubbles through electrostatic interaction via incorporation of cationic lipids into the stabilizing wall material. In our experience the microbubbles may become unstable when much more than around 10% of the shell forming lipid is subsitituted with the cationic lipid (Unger, unpublished data). Sirsi, Borden and Jin have increased the loading capacity of microbubbles for genetic materials by attaching cationic polymers (e.g. polyethyleneimine) to the surface of the microbubbles [43–45]. Using this approach it may be possible to delivery larger quantities of genetic material or gene-based drugs with UTMD. Drugs or genes can be condensed into nanoparticles and then bound to the surface of microbubbles. Nanoparicles with functionality for other forms of imaging (e.g. nuclear medicine or MRI) can be incorporated into the nanoparticles that are bound to the microbubbles [46,47]. A wide variety of drugs can be incorporated into liposomes. Klibanov et al. have attached drug containing liposomes to microbubbles for UTMD [48]. So a number of approaches are possible for increasing drug loading, loading different classes of drugs and using UTMD for localized release and delivery. As the complexity of the delivery system increases the needs for chemical characterization, quality control and toxicological study increase, potentially creating challenges to clinical translation.
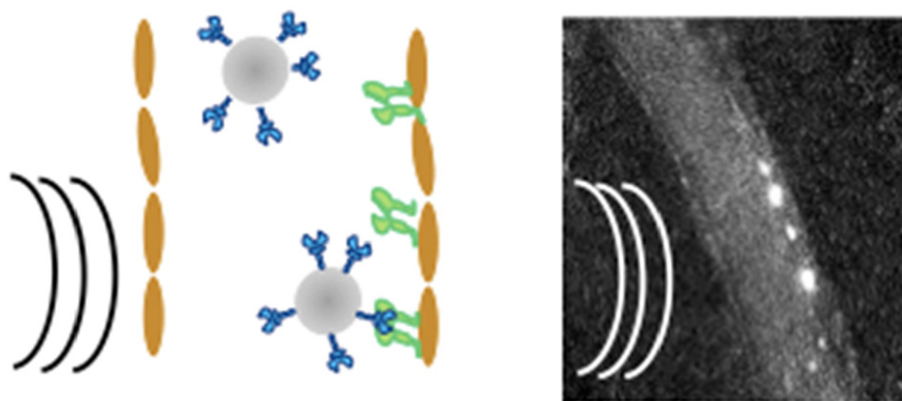
Fig. 3. Radiation force. Ultrasound is applied to a tissue containing blood vessels and encounters targeted microbubbles bearing ligands targeted to endothelial epitopes. The radiation force of ultrasound pushes the microbubbles towards the surface of the vessel increasing the interaction of the microbubbles with the endothelial cells resulting in increased binding of the microbubbles to the targeted endothelial cells. Images courtesy of Kathy Ferrara, UC Davis and Paul Dayton, University of North Carolina.

2. Sonothrombolysis

Vascular thrombosis is responsible for most cases of ischemic stroke and myocardial infarction as such may be considered the single greatest cause of death [49]. Rapid restoration of blood flow is necessary to improve outcomes in stroke and heart attack. Ultrasound can be used with microbubbles for sonothrombolysis, to relatively non-invasively dissolve blood clots and restore blood flow [50–55].

Fig. 5 depicts sonothrombolysis in acute vascular occlusion caused by clot [55].

2.1. Basic principles

Cavitation of microbubbles is an important mechanism underlying sonothrombolysis [56]. There is an effect of ultrasound alone without microbubbles, using ultrasound power levels within the range as allowed by the FDA for diagnostic imaging [57], but the effect is enhanced by the presence of microbubbles [52–54]. In sonothrombolysis, pulsing of high-energy ultrasound is generally punctuated by periods of time without high-energy pulsing; during these intervals, low mechanical index ultrasound imaging may be performed to monitor influx of fresh microbubbles into the region of thrombosis [53]. The periods without high-energy pulsing allow for entry of fresh microbubbles into the ultrasound field.

2.2. Stroke summary

Stroke is the 3rd leading cause of death in the US and the single greatest cause of expenditures for long-term medical care [58]. There are two kinds of stroke, ischemic (due to blockage of a blood vessel — usually by thrombus) and hemorrhagic (about 20% of strokes), e.g. by rupture of an aneurysm. Prior to treatment of ischemic strokes (80% of strokes) hemorrhage is excluded by CT scan or MRI scan. The only approved drug to treat stroke is tissue plasminogen activator (t-PA) [59,60]. t-PA is only approved by the FDA for administration for the time period of the first 3 h following stroke, although there is consensus among many neurologists that it should be given up to 4.5 h following stroke [60]. Because of risk of bleeding and other factors, t-PA is only administered to less than 10% of patients with stroke [61,62]. Better methods of stroke treatment are needed to improve outcomes [63].

Andrei Alexandrov led the Combined Lysis of Thrombus in Brain Ischemia Using Transcranial Ultrasound and Systemic t-PA (CLOTBUST) trial to see if ultrasound could improve outcomes in stroke patients being treated with lytic therapy [57]. CLOTBUST prospectively enrolled 126 patients into two treatment arms in a multicentre randomized trial. All patients received standard IV t-PA therapy (0.9 mg/kg — maximum 90 mg) with 10% given as a bolus and 90% by continuous infusion. Therapy was initiated within 3 h of the onset of stroke, either with continuous Doppler ultrasound (the target group) or placebo monitoring (the control group). Ultrasound was applied with transcranial Doppler at 2 MHz, using equipment and parameters approved by the FDA. Emitted power was set at the maximum permissible level of 750 mW/cm^2. Sample volumes, or gates of insonation, were set at 3 to 6 mm for power-motion Doppler units and 10–15 mm for single-channel transcranial Doppler units. Early recanalization of arterial occlusion was seen more significantly in the target group exposed to continuous transcranial Doppler (TCD) than the control group (p = 0.03). Complete recanalization within 2 h was seen in 29 (46%) of the target
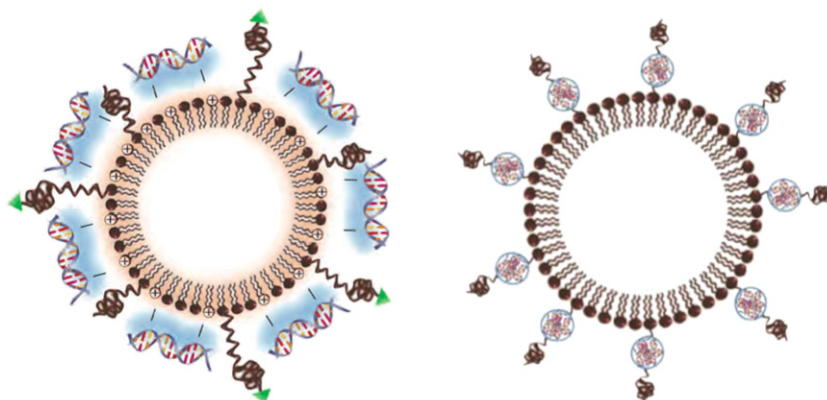

Fig. 4. Two different examples of microbubbles designed for gene delivery with UTMD.
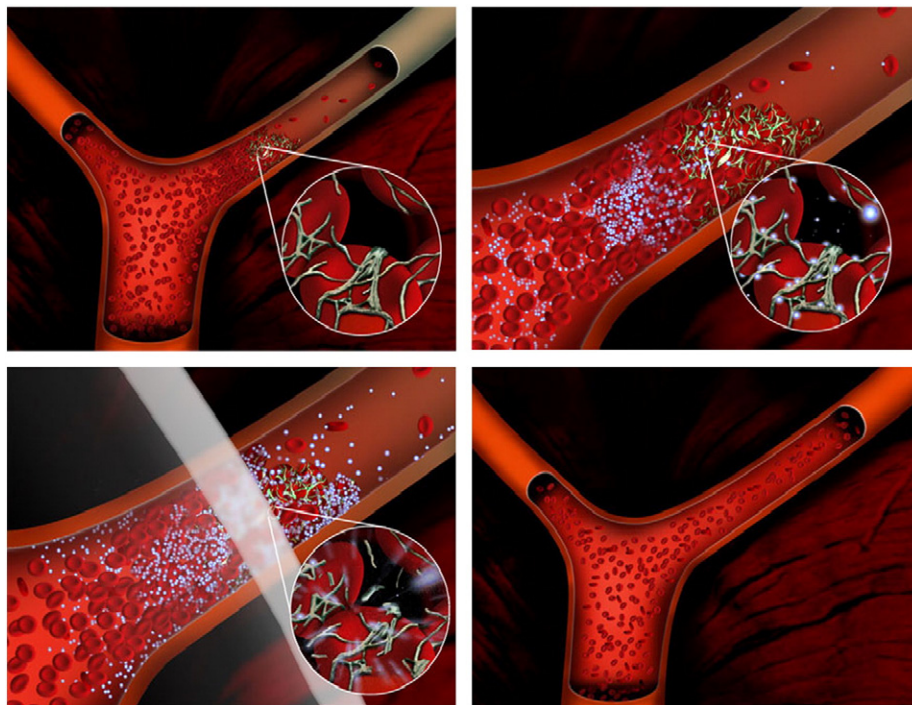
Fig. 5. Microbubble-enhanced sonothrombolysis of occlusive clot. The upper left image depicts a vascular occlusion caused by a clot that comprises fibrin, platelets and red blood cells. Microbubbles are administered (e.g. by IV injection) and accumulate in the clot. Ultrasound is applied (lower left image) and cavitates the microbubbles dissolving the blood clot and restoring flow (lower right).
Reference [55], with permission of Wiley and Sons.

group and 11 (18%) of the control group (p < 0.001). Both clinical recovery and complete recanalization were observed in 16 (25%) of the target group and 5 (8%) of the control group (p = 0.02). There was a trend to a higher rate of functional recovery in the target group, which may have been significant had more patients been enrolled in the study. There were similar rates of intracranial hemorrhage in target and control groups (i.e. no evidence that TCD increased the rate of hemorrhage).

Because it was well known that microbubbles increased the rate of clot dissolution with ultrasound it was logical to incorporate microbubbles into the treatment regime. In addition, Molina et al. had published a study showing favorable results with microbubbles and TCD to treat stroke [63]. A prospective pilot study using Definity microbubbles was performed [64]. Fifteen subjects were randomized 3:1 to Target, n = 12 or Control, n = 3. A standard IV infusion of 0.9 mg/kg of t-PA was administered to all subjects. TCD was applied continuously for 2 h to the target group. Perflutren, 2.8 ml was diluted in 100 cm^3 of normal saline ad infused for 60 min during the TCD application. TCD was at 2 MHz and 720 mW. Spectral waveforms were obtained at 0, 30, 60, 90 and 120 min from the initiation of treatment. After treatment a total of asymptomatic hemorrhages were found: 3 in target (25%) and 1 in control (33%) subjects. The rates of any recanalization within 2 h after t-PA bolus for TCD + t-PA + MB versus t-PA in CLOTBUST were: complete 50% (6/12) versus 18% (11/63), partial 33% (4/12) versus 33% (21/63), and none 17% (2/12) versus 49% (31/63).

After obtaining favorable results for treatment of stroke with sonothrombolysis using perflutren the Transcranial Ultrasound in Clinical Sonothrombolysis (TUCSON) trial was performed [56]. TUCSON was a prospective study similar in design to the pilot study but using MRX-801 rather than perflutren. MRX-801 was comprised of phospholipid coated microbubbles, similar to perflutren, but with higher lipid concentration and larger number of microbubbles. The study protocol for administration of t-PA, application of TCD and administration of microbubbles was similar to the pilot study. The study was designed to enroll patients in 4 consecutive cohorts (4 dose tiers in escalating fashion: 1st tier infusion of 1.4 ml of MRX-801; 2nd tier, infusion of

2.8 ml, 3rd tier, 5.6 ml and 4th tier, 11.2 ml of MRX-801) each comprising 12 patients in the target group and 6 in the control group. A total of 35 patients were enrolled in the study. After 3 cases of symptomatic intracranial hemorrhage in the 2.8 ml dose group the study was discontinued. The median time to any recanalization (as determined by TCD) was shorter in the treatment groups and the difference from control was almost significant (p = .054). There was a trend towards greater functional independence in the treatment groups compared to control.

The results from the pilot study with Definity and the TUCSON trial show that microbubbles decrease the time to arterial recanalization as well as increase the rate of recanalization. The TUCSON trial suggests that low doses of microbubble used in sonothrombolysis may be safe but that higher doses of microbubbles when co-administered with t-PA may increase the rate of symptomatic intracranial hemorrhage [65]. The rate of SICH from t-PA is about 5–6% in stroke patients [59]. In the TUCSON trial there was a rate of hemorrhage of 27% in the cohort of patients receiving 2.8 ml of the microbubbles and 0% in the group receiving the 1.4 ml dose.

Subsequent to completion of the TUCSON trial Culp et al. completed a number of studies in an embolic model of acute ischemic stroke in rabbits [66–68]. Culp et al. showed that US + perflutren significantly decreased stroke volume compared to control without hemorrhage [67]. Culp et al. also showed that t-PA + US + perflutren did not increase hemorrhage compared to t-PA alone [66–68]. Culp's et al. results suggest that clinical studies of US + microbubbles without t-PA merits study in patients who are not candidates for t-PA [67]. As noted above, due to window of time for which t-PA is indicated and risk factors for bleeding, most patients are not candidates for t-PA. Sonothrombolysis with US + microbubbles without t-PA could afford a treatment option for patients for whom t-PA is contraindicated. Additional studies of sonothrombolysis in stroke are warranted.

Certainly the ultrasound parameters employed for sonothrombolysis treatment of stroke are important for optimizing efficacy as well as minimizing the risk of hemorrhage [69]. The TRUMBI trial (transcranial low-frequency ultrasound mediated sonothrombolysis in brain ischemia)

used 300 kHz ultrasound in association with t-PA [70]. The trial was stopped prematurely when 13 of 14 patients in the treatment group developed intracranial hemorrhage versus 5 of 12 in the t-PA group [70]. The pattern of hemorrhage was atypical in the ultrasound group with bleeding in the subarachnoid or in the ventricular space outside the brain or at remote locations outside the infarct core [70]. The use of MRI in this study rather than CT may account for the higher detection of hemorrhage than typical in the control group but the significantly higher rate of hemorrhage in the ultrasound treatment group as well as the presence of hemorrhage in atypical locations indicates that ultrasound was responsible for the increase in bleeding. The investigators speculated that reverberations of the long wavelength of the ultrasound occurred inside the head leading to hot spots of energy [70]. Also the transducer employed in the TRUMBI trial exposed a much larger portion of the brain to ultrasound energy that the 1-cm probe used in the CLOTBUST trial described above, where the rate of hemorrhage in the t-PA + ultrasound group was no greater than in the t-PA control group [57].

Bor-Seng-Shu et al. conducted a meta-analysis of the published studies of sonothrombolysis for acute ischemic stroke with a systematic review of randomized controlled trials [71]. The authors identified four trials that met the criteria of being truly randomized; 2 trials evaluated the effect of transcranial Doppler (TCD) ultrasonography on sonothrombolysis, and 2 addressed transcranial color-coded duplex (TCCD) ultrasonography [71]. The frequency of ultrasound varied from 1.8 to 2 MHz [73]. The TRUMBI trial did not meet the criteria of being a randomized trial because patients were sequentially allocated to the treatment groups. There were no differences in intracranial hemorrhage rates between the sonothrombolysis and control (t-PA only) groups of the studies, except for the TUCSON study described above where the higher 2.8 cm^3 dose of microbubbles was used (hemorrhage was no higher than control in the cohort of patients receiving 1.4 cm^3). From their meta-analysis, the authors concluded that sonothrombolysis combined with t-PA did not lead to an increase in symptomatic intracranial hemorrhagic complications when performed with TCCD or TCD [71]. Two of the studies demonstrated that patients treated with ultrasound + t-PA had statistically significant higher rates of recanalization than patients treated with t-PA alone [72]. Complete arterial recanalization rates varied from 15% to 67% in the sonothrombolysis group and from 11% to 33% in the t-PA control groups [72]. Two of the studies, one using TCD and the other using TCCD, demonstrated that patients treated with ultrasound + t-PA had statistically significantly higher rates of both complete recanalization and neurological improvement than those treated with t-PA alone [57,71,72].

MRI guided high intensity focused ultrasound has also been explored as a potential means of treating stroke [73]. Burgess et al. used high-intensity focused ultrasound (HIFU) for dissolution of clots in a rabbit model of embolic stroke. The highest intensity of ultrasound tested, 550 W, at 1.5 MHz was most effective at clot dissolution, but hemorrhages also occurred as the acoustic power was increased [73]. It is possible to use a wide variety of acoustic parameters to treat stroke but the greatest clinical experience has occurred with TCD and TCCD. A modified TCD-based system is currently being tested clinically [74]. A Phase 3, randomized, placebo-controlled, double-blinded trial of combined lysis of thrombus with ultrasound and systemic t-PA is currently being evaluated for the emergent revascularization of acute ischemic stroke referred to as the CLOTBUST-ER trial [74]. This trial will not evaluate the use of microbubbles due to the added regulatory complexity of combing microbubbles into the clinical trials.

2.3. Cardiac summary

Myocardial infarction is responsible for more deaths than any other single disease [49]. The causative mechanism is usually plaque rupture with formation of thrombus in the coronary artery [75]. Primary angioplasty and stenting are accepted as standard therapy, but due to unavailability of emergent interventional coronary care [76], many patients in the US are treated with medical therapy rather than primary coronary intervention. Even with primary angioplasty there still may be regions of no-reflow in the coronary microcirculation, which may be due to microvascular thrombi that have propagated downstream from the primary coronary lesion [77]. Sonothrombolysis might be useful to restore flow in the epicardial circulation in patients who do not receive primary angioplasty. In patients who receive primary angioplasty, sonothrombolysis might still be useful if it eliminated the region of no-reflow in the coronary circulatory bed. A number of studies have been performed evaluating microbubble-enhanced sonothrombolysis for treatment of MI [78–85].

To test the hypothesis that sonothrombolysis would improve the no-reflow phenomenon a study was performed in 26 pigs with acute thrombotic occlusions of the left anterior descending (LAD) coronary arteries [82]. In 12 of the pigs pre-existing atherosclerotic lesions were created by balloon angioplasty injury of the LAD on day 1 followed by a high fat diet. Coronary artery thrombotic occlusions were created in the 14 normal pigs by simulating the triad of Virchow. Endothelial injury was created by advancing a balloon catheter in the LAD, inflating the balloon, and then injecting clotted blood into the LAD. Once LAD occlusion occurred it had to persist for >20 min prior to treatment. Subsequent to confirmation of LAD occlusion, 650 mg of aspirin was administered per nasogastric tube, followed by an intravenous heparin bolus (80 mg/kg) and a bolus injection of half-dose fibrinolytic agent (0.25 mg/kg tenecteplase or 1 mg/kg tissue plasminogen activator; Genentech, South San Francisco, CA). The normal pigs were then randomized to receive either no additional treatment (the control group, subsequently referred to as group I; n = 7) or continuous IV infusion of MRX-801 (NuvOx Pharma Inc., Tucson, AZ) with intermittent high-MI impulses applied whenever microbubbles were visualized within the risk area (group II). In the 12 atherosclerotic pigs, coronary artery thrombi were created at 52 ± 21 days after the day 1 balloon injury using the same protocol described for groups I and II. Subsequently, the pigs received either no additional treatment (group III) or the same MRX-801 infusion with intermittent high-MI impulses applied to the risk area (group IV). The microbubble infusions were prepared by diluting 2 ml of MRX-801 in 100 ml of 0.9% saline and infusing at a rate of 2.5 to 3.0 ml/min. In pigs randomized to receive ultrasound, real-time low-MI biplane images were obtained using a matrix-array 1.6-MHz 3D transducer (power modulation at an MI of 0.2; Philips Medical Systems, Andover, MA), which permitted visualization of infarct size. A 3D array of high-MI impulses (MI, 1.2) was delivered from the same transducer at a frame rate of 5 Hz for 5 s (a total of 25 frames) after the visualization of microbubbles within any portion of the peripheral or central portions of the risk area (defined by the extent of the wall thickening abnormality) [82]. The transducer and echocardiography images are shown in Fig. 6.

In all pigs, epicardial recanalization was assessed by angiography using left main coronary artery injections of 5 ml of iodinated contrast at 30, 60, and 90 min after the initiation of treatment protocols. Twelve-lead electrocardiography was performed at baseline before treatment and at 30, 60, and 90 min. Maximal ST-segment elevation was compared at each time point. Wall thickening within the central portion of the risk area on a two-dimensional short-axis view (midpapillary muscle level) was determined by a blinded reviewer, who measured end-diastolic and end-systolic wall thickness before treatment and at 60 min into treatment [82].

The study in pigs described below shown in Figs. 7 and 8 shows that sonothrombolysis using intermittent high MI pulses guided with low MI imaging using a 3-D transducer is effective at improving myocardial blood flow and decreasing infarct size, even when the epicardial circulation is not restored. This work has evolved into a randomized pilot study in 10 patients performed by Otto Kamp and his colleagues in the Netherlands showing that pre-angioplasty sonothrombolysis did not lengthen the time to balloon angioplasty and that the treatment appeared to be safe [85]. A randomized prospective clinical trial is
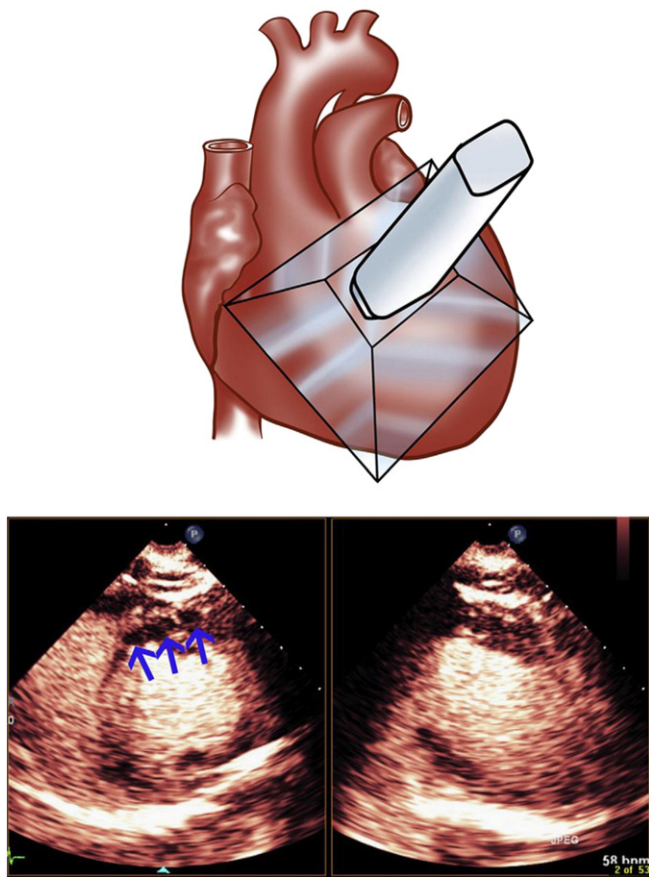
Fig. 6. Depiction of the transthoracic coverage of the 3D transducer. The 3D transducer was used for the application of guided high-MI impulses after acute LAD thrombotic occlusion [82]. Blue arrows depict the hypoperfused zone identified with biplane low-MI imaging after LAD thrombotic occlusion.

presently underway in Amsterdam, NL (PI Kamp). In this study patients will receive medical therapy similar to that described above in the porcine study and all patients will undergo angioplasty. Patients randomized to sonothrombolysis will have the procedure performed prior to angioplasty. Area of no-reflow in coronary circulatory and ultimate infarct size will be compared between angioplasty alone and angioplasty + sonothrombolysis groups. A similar randomized prospective study is now also being conducted in Brazil [86].

3. Targeted microbubbles

A number of preclinical studies have shown that microbubbles hold great potential as agents for molecular imaging. In this review we concentrate on potential therapeutic applications of targeted microbubbles. Most of the work on targeted microbubbles has used lipid-coated microbubbles and followed variations of a basic design. Lipids bearing polyethyleneglycol (PEG) are incorporated into the lipid shell surrounding the microbubble. The purpose of the PEG is to prevent binding of the microbubbles to serum proteins and other materials that would otherwise shorten the serum half-life of the microbubbles [87]. Targeting ligands are generally affixed to the free ends of the PEG chains to direct the microbubbles to a given target. Targeted microbubbles usually bear thousands of ligands on the surface of the microbubbles. Cooperative binding of multiple ligands to a target may increase the affinity of the microbubbles to the target site [88]. Microbubbles binding to sites with high blood flow are subjected to shear stress related to flow rate and the size of the microbubbles [89]. The "on/off rate" of the ligand for its target and stability constant of the ligand for its target are all important factors in the design of targeted microbubbles [90]. If ligands can be designed to target more than one epitope on a target (heteropolyvalency) this may increase the strength of cooperative binding.

Recently a microbubble targeted to the VEG-fR2 receptor (BR-55) has been developed and has entered clinical trials [18]. BR-55 contains a lipopeptide which has a heterodimeric peptide that targets two different epitopes on the VEG-fR2 receptor. By non-competitively binding two different sites this strategy results in firm binding even under conditions of high shear stress. Most work on BR-55 has involved imaging angiogenesis associated with cancer. A VEG-fR2 targeted agent,
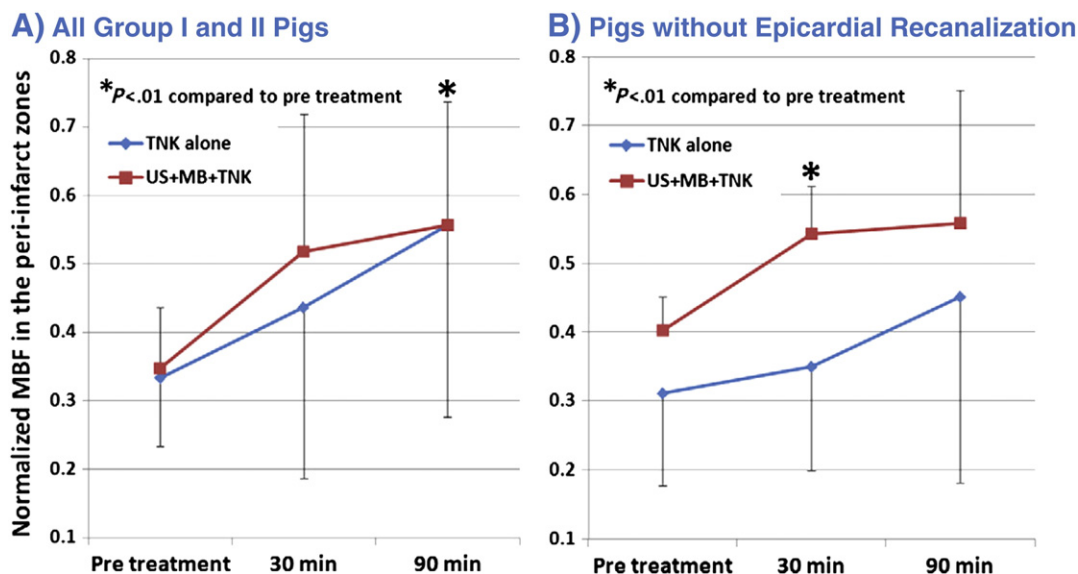

Fig. 7. (A) Changes in peri-infarct MBF in group I and group II pigs before and after randomized treatment to either tenecteplase (TNK) alone or TNK with diagnostic ultrasound (US) and intravenous nontargeted microbubbles (MBs) (group II). The improvement in peri-infarct MBF occurred was seen at 30 min into treatment, even in those without epicardial recanalization (B) [82].
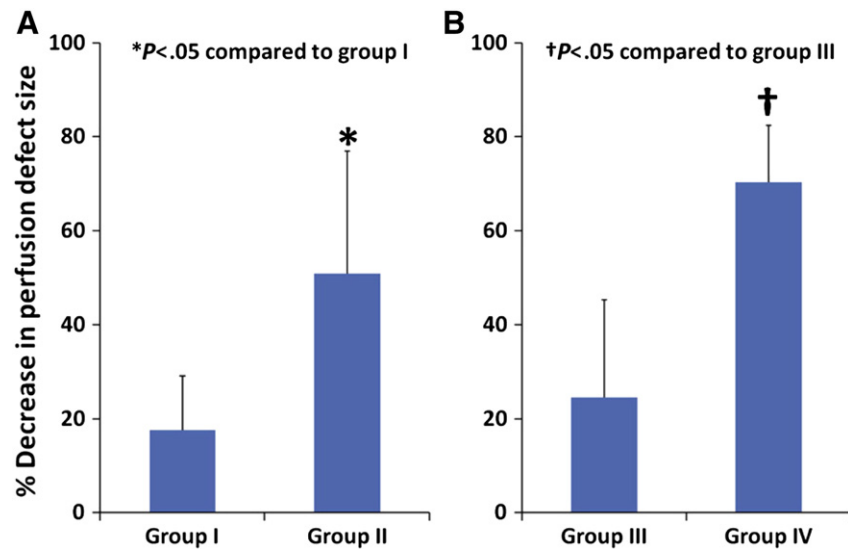Reference [82], with permission of Elsevier.

Fig. 8. Improvement in planimetered defect size. Improvement in planimetered myocardial infarct defect size was determined at plateau contrast intensity (ultimate infarct size) in the group II (A) and group IV (B) pigs treated with 3D ultrasound and microbubbles [82]. The improvement in defect size in group II pigs was observed even without epicardial recanalization in five of the seven pigs treated.
Reference [82], with permission of Elsevier.

however, might also be useful in imaging associated with vascular re-modeling in heart disease and in characterizing vulnerable plaque [91].

3.1. Accessible targets

Table 2 lists some of the cardiovascular diseases that might be targets for molecular imaging, therapy and drug delivery with ultrasound.

In all of the examples listed above, the targeting ligands are affixed to the surface of the microbubbles with PEG linkers, with the exception of phosphatidylserine (PS) coated microbubbles. Activated macrophages and monocytes have receptors for PS [26]. PS is a phospholipid that is normally expressed on the internal leaflet of the lipid bilayer surrounding cells. When cells undergo apoptosis, PS is translocated to the external leaflet of the dead cells [97,98]. Macrophages avidly phagocytose PS. Monocytes also internalize PS coated microbubbles.

3.2. Studies of sonothrombolysis with targeted MB

The rationale behind sonothrombolysis with targeted microbubbles is two-fold [81,99,100]. Firstly thrombus targeted microbubbles can be used as diagnostic imaging agents to detect and localize the clot. Secondly, by binding the microbubbles (cavitation nuclei) directly to the clot, ultrasonic induced cavitation may be more effective in dissolving the clot. As noted in Table 2, targeted microbubbles may be directed to clot by using ligands directed to receptors on activated platelets or on fibrin.

In vitro studies of sonothrombolysis generally have shown enhanced efficacy in clot lysis for sonothrombolysis using clot-targeted microbubbles compared to non-targeted microbubbles. Fig. 9 shows results from in vivo sonothrombolysis using platelet-targeted microbubbles compared to non-targeted microbubbles [81]. In this study occlusive thrombi were created in the LAD of pigs, the microbubbles administered intravenously and ultrasound applied transcutaneously to the heart. Serial angiography was performed to verify arterial recanalization. As shown in Fig. 7, early arterial recanalization was significantly better with the targeted versus the non-targeted microbubbles (Reference [81], with permission of Wolters Kluwer Health).

Clot-targeted microbubbles will likely require extensive animal testing prior to human studies. It does appear that there are advantages to the targeted microbubbles, but current FDA-approved microbubbles are also efficacious and might be used in clinical trials of sonothrombolysis more easily than the clot-targeted microbubbles. The clot-targeted microbubbles, however, have potential utility as theranostic agent to diagnose and treat clot. The targeted microbubbles used in sonothrombolysis may help to restore blood flow more quickly. Since cavitation nuclei are presumably more effectively concentrated in the clot, the targeted microbubbles may also enable a lower energy level of ultrasound to be used effectively for sonothrombolysis, e.g. potentially below the threshold level for inertial cavitation. A lower energy level of ultrasound could help to minimize any potential adverse bioeffects. Targeted microbubbles have also been prepared to encapsulate t-PA [101]. If targeted microbubbles could be used to deliver

Table 2
Potentially accessible targets for molecular imaging with ultrasound.

| Disease	Target	Potential ligands	Therapeutic application
Myocardial ischemia	P-selectin, E-selectin [92]	P-selectin Glycoprotein ligand (YPSL), Peptides, antibodies	Imaging ischemic memory, guiding therapy
Vulnerable plaque	ICAM-1, VCAM-1 [93]	Peptides, antibodies	Diagnosis and treatment
Vulnerable plaque	von Willebrand factor [94]	Glycoprotein 1B	Diagnosis and treatment
Vascular thrombosis	Platelets (GPIIBIIA) [95] Fibrin	Peptides Peptides and antibodies	Diagnosis and sonothrombolysis
Vascular remodeling	VEG-f receptor [18]	VEG-f, peptides, antibodies	Diagnosis, drug delivery
Vascular inflammation	ICAM-1, VCAM-1 Activated macrophages, monocytes [96]	See above Phosphatidyl-serine	Diagnosis, drug delivery
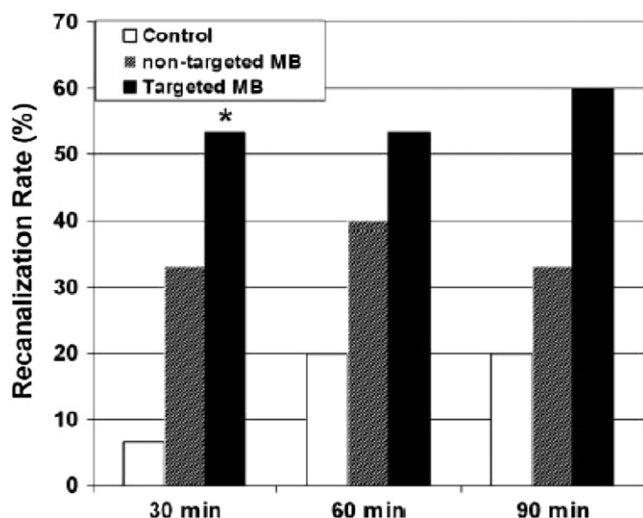
Fig. 9. Pigs randomized to diagnostic ultrasound and targeted intravenous microbubbles (MBs) had significantly higher recanalization rates than control (lytic therapy alone) at 30 min of treatment. Non-targeted intravenous microbubbles achieved a similar recanalization rate (50%) at 60 min. *p = 0.02 compared with control [81].

thrombolytic agents directly to clot and employed with UTMD, this might afford a revolutionary new paradigm in the treatment of vascular thrombosis.

3.3. Endothelial epitopes as targets

As noted in Table 2, a variety of diseases might be assessed by targeting epitopes on endothelial cells. Fig. 10 shows an example of imaging ischemic memory with p-Selectin targeted microbubbles [102]. In this experiment microbubbles were prepared with antibodies targeted to p-Selectin and recombinant YSPSL [102]. The mouse cremaster muscle was exteriorized and studied with optical microscopy. Studies were

also performed in a model of myocardial ischemia in the mice. The targeted microbubbles enabled detection of and quantification of p-Selectin expression on endothelial cells in heart and muscle tissues after ischemia. Compared to WBCs (described in Section 3.4) p-Selectin targeted microbubbles may enable detection of less severe degrees of ischemia.

Unger et al. recently studied e-Selectin targeted microbubbles in a model of uveitis [103]. In these studies a peptide that binds to e-Selectin was affixed to the microbubbles. The targeted microbubbles bound to inflamed retinal endothelial cells in vivo and the microbubbles were internalized by the inflamed retinal endothelial cells [103]. Internalization of the microbubbles suggests potential for drug delivery. Microbubbles have been designed to carry dexamethasone pro-drug for delivery to the inflamed endothelial cells.

3.4. WBC's (immune/phagocytic cells as carriers)

White blood cells will internalize microbubbles and carry the microbubbles to the site of inflammation. This can be used to diagnose sited of vascular inflammation as shown in Fig. 11 [104]. By incorporating phosphatidylserine into the lipid coating the microbubble the rate at which the microbubbles are internalized by the white blood cells might be increased [104]. WBC-targeted microbubbles might be used for drug delivery (e.g. anti-inflammatory drugs).

4. Gene delivery

In general, microbubbles have a limited capacity to contain a payload of drug. In order for drug carrying microbubbles to be used effectively, the drug should probably be highly active, i.e. require a low dose so that a small amount of drug could be package into or onto microbubbles. Genetic medicines, e.g. plasmid DNA, and si-RNA, require low doses and may be highly effective when delivered with microbubbles and ultrasound. For plasmids to be expressed they must generally be delivered intracellularly and to the cell nucleus. Some genetic based medicines such as si-RNA not only are active in the cytosol but also must be
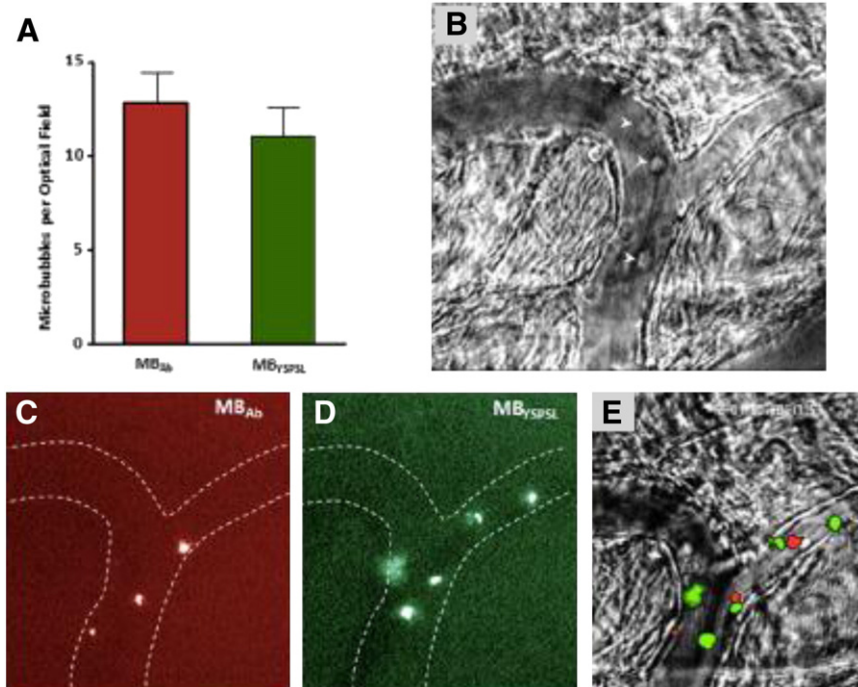

Fig. 10. Microbubble attachment to mouse cremasteric venules. (A) Mean ± SEM number of retained microbubbles per optical field. Intravital microscopy images of the cremaster muscle illustrate (B) converging venules with rolling leukocytes (arrowheads) on bright field microscopy, (C) venular adhesion of dioctadecyltetramethyl-indocarbocyanine-labeled MBAb, (D) venular adhesion of dioctadecyloxacarbocyanine-labeled MBYSPSL, and (E) merged images [102].
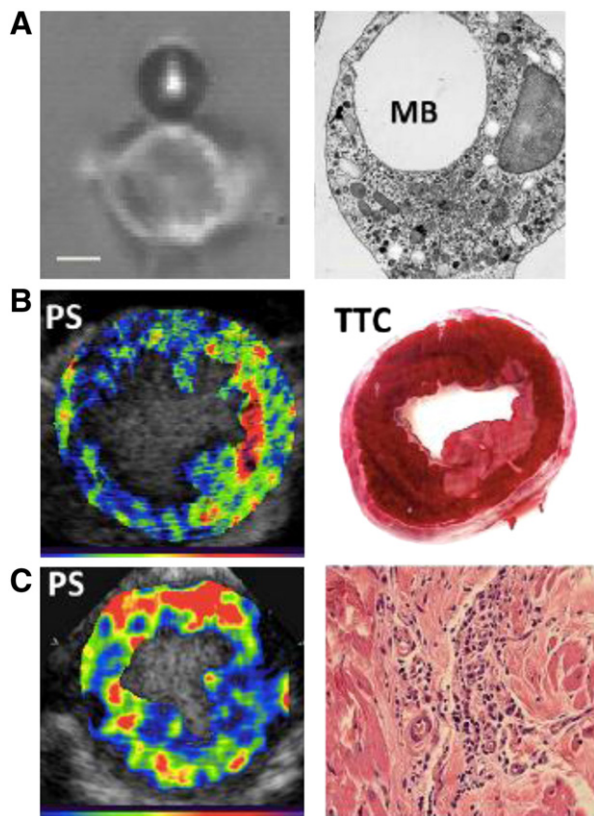Reference [102], with permission of Elsevier.

Fig. 11. Ischemic myocardial disease. Ultrasound imaging of inflammation in ischemic myocardial disease is detected by interactions between leukocytes and lipid-shelled microbubbles (MBs) containing phosphatidylserine [104]. (A) Light microscopic image demonstrating attachment of an MB to the surface of an activated neutrophil (left) and transmission electron microscopy demonstrating MB internalization (right). (B) Short-axis images from a dog 2 h after circumflex ischemia and reperfusion demonstrating myocardial enhancement several minutes after IV injection of PS-containing MBs and corresponding histology demonstrating region of infarction. (C) Contrast echocardiography in the short axis using PS-containing MBs demonstrating leukocyte recruitment in a model of progressive ischemic left ventricular dysfunction caused by ameroid constrictors (left) and corresponding hematoxylin and eosin staining from the anterior myocardium illustrating perivascular leukocyte infiltration (right) [104].
Reference [104], with permission of Elsevier.

delivered intracellularly. Virus-based delivery systems may be highly efficient vectors, i.e. enable efficient gene delivery with high level of expression. Viruses, however, can be immunogenic and cause allergic reaction [105]. Retroviruses also have oncogenic potential [106]. Because of these limitations, microbubbles afford a potentially attractive alternative to virus for gene delivery.

4.1. Brief review of UTMD in cardiovascular system

Ultrasound and ultrasound targeted microbubble destruction (UTMD) have been used by a number of different researchers for gene delivery to the cardiovascular system [107–114]. The microbubbles are destroyed within the ultrasonic field to deliver genetic based medicines to the target tissue. Microbubbles that bind the genetic materials are probably more effective than microbubbles that are co-administered, but do not bind the genetic medicines in UTMD to provide gene delivery to the target cells with high levels of expression of the gene [115]. The approved phospholipid and albumin-coated microbubbles probably do not strongly bind plasmid DNA. There is some controversy in this regard as at least one researcher has reported binding of DNA by perflutren [116]. In our experience, however, perflutren did not bind DNA (Unger et al. [103]) but different conditions in the binding experiments might account for the lack of binding in our experiments. Most of the studies of microbubbles for UTMD gene delivery have used either the

existing FDA approved microbubbles or cationic microbubbles. Cationic microbubbles are prepared by incorporating positively charged lipid into the membrane surrounding the microbubble [117,118]. DNA is a polyanion and will then bind to the cationic microbubbles. Another way of loading DNA onto the microbubbles is to do layer by layer assembly, a method that might allow for larger amounts of DNA to be loaded onto the microbubbles [119]. As noted earlier, polymeric microspheres have also been prepared to encapsulate DNA [41]. Microbubbles have also been prepared using cationic polymers on the surface to increase the loading capacity of the microbubbles for DNA [43–45]. Cationic microbubbles, or other specific microbubble constructs that are designed to bind the genetic drug, are probably more effective for gene delivery than neutral or anionic microbubbles but the already approved microbubbles might have advantages for easier entry into clinical trials.

Fujii et al. used perflutren for gene delivery to treat myocardial infarction in a mouse model [113]. They delivered genes for green fluorescent protein (GFP), vascular endothelial growth factor (VEG-f) and stem cell factor (SCF) using perflutren and UTMD (see Fig. 12). They showed expression of GFP and protein in the heart, increased migration of stem cells into hearts treated with gene delivery with UTMD and improved myocardial repair in treated animals compared to controls [113].

The experiment shown above by Fujii et al. suggests the potential of UTMD gene delivery to treat myocardial infarction using perflutren [113]. Greater efficacy might be attained using microbubbles that not only bind DNA but also carry targeting ligands to bind to the surface of the target cells or the endothelial cells lining the vessels within the target tissue as shown in Fig. 13. Xie et al. conducted a study using cationic microbubbles to bind DNA [118]. Targeting ligands to ICAM-1 and p-Selectin were attached to the surfaces of the microbubbles [118]. Binding plasmid DNA to the microbubbles did not affect the capacity of the microbubbles to bind to inflamed endothelial cells in cremaster muscle. UTMD was used to deliver the plasmid for luciferase reporter gene. The targeted microbubbles were significantly better than the non-targeted microbubbles at attaining gene expression at low MI [118]. Both targeted and non-targeted microbubbles had similar efficacy at MI = 1.0 and 1.8 but capillary hemorrhages were present at higher MI.

The above experiment by Xie et al. shows that targeted microbubbles binding DNA may enable a lower MI of ultrasound to be used in UTMD [118]. A number of other studies have been performed with UTMD for gene delivery to the cardiovascular system [120–124]. Studies have shown that UTMD can be used to improve engraftment of endothelial progenitor cells, mesenchymal and cardiac progenitor cells [119–122]. Most of the studies to date have been in small animal models. Of note, any of the microbubbles specifically designed to deliver genetic materials will have to undergo extensive testing prior to any eventual human studies. Targeted microbubbles for UTMD gene delivery hold great promise and as the field evolves we might expect these agents to enter formal development. The most developed UTMD gene delivery system is probably the one under development for diabetes described below.

4.2. Gene delivery to treat diabetes

Diabetes represents an enormous medical problem, affecting about 25.8 million Americans — 8.3% of the US population [123]. Adults with diabetes have heart disease death rates about 2 to 4 times higher than adults without diabetes [124]. The risk for stroke is also 2 to 4 times higher among people with diabetes [125]. Work on UTMD gene delivery to treat diabetes has progressed relatively far compared to most of the other areas of gene delivery [126–128].

Grayburn et al. have developed a gene therapy approach using an insulin specific promoter RIP 3.1 to drive expression of the gene NeuroD [126,127]. The plasmid DNA is bound to cationic microbubbles and infused IV [126,127]. UTMD is accomplished by applying ultrasound to the pancreas using a clinical transducer. The pancreatic islets are destroyed by streptozotoxin and UTMD is performed two days later.
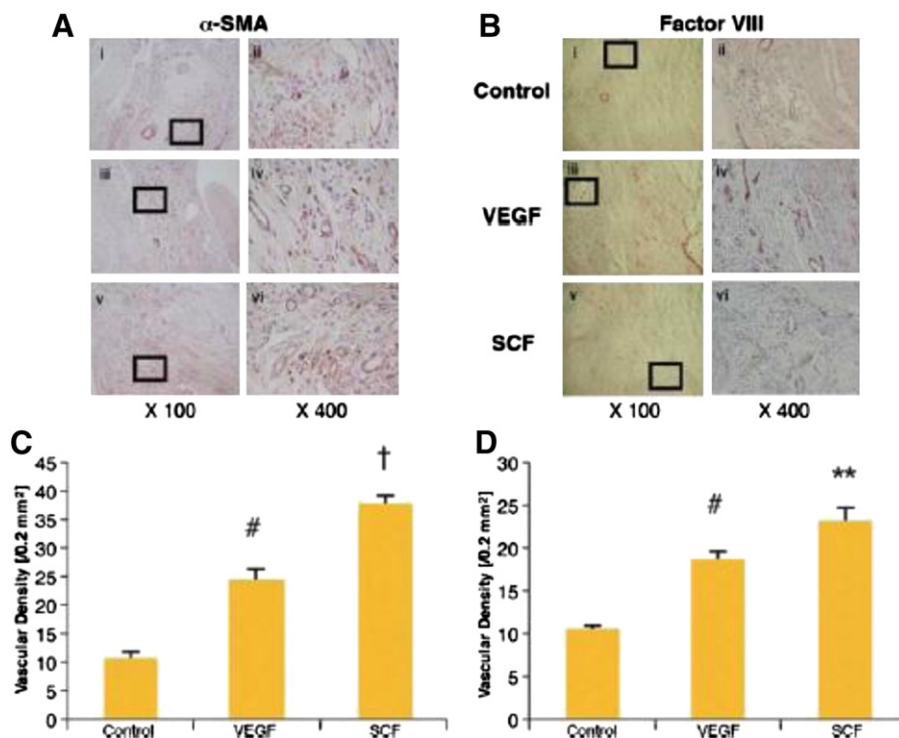
Fig. 12. UTMD gene delivery. Immunohistological evaluation of arteriolar and capillary densities (A, B) [67]. Representative micrographs (low magnification, with areas of interest [black boxes] enlarged in adjacent columns) illustrating immunostaining with antibodies against α-smooth muscle actin (α-SMA, to identify arterioles, A) or Factor VIII (to identify capillaries, B) at 14 days after ultrasound-targeted microbubble destruction in the infarct region of myocardial tissue sections from mice transfected with empty plasmid (control group) (A, B: i to ii), vascular endothelial growth factor (VEGF) (A, B: iii to iv), or stem cell factor (SCF)(A, B: v to vi). (C to D) Quantification of arteriolar (C) and capillary (D) densities in the myocardial infarct regions of all 3 groups. **p < 0.01 versus all groups; #p < 0.001 versus control group; †p < 0.001 versus all groups [113]. Reference [113], with permission of Elsevier.

Fig. 14 shows results from UTMD gene delivery in rats. Histological study of the pancreas tissue shows regeneration of islets in the pancreas of diabetic rats. By day 3 following UTMD there is normalization of blood glucose levels and restoration of insulin levels. C-peptide levels, a marker of the volume of beta cell islets that also returns to normal in animals treated with UTMD using RIP 3.1 and NeuroD. Co-administration of other genes, may further improve result for gene therapy treatment of diabetes. Delivery of the gene for vascular endothelial growth factor has been shown to improve revascularisation and restoration of euglycaemia after human islet transplantation into mouse liver [128].

To advance the development of UTMD gene delivery to treat diabetes, studies were performed in baboons. Plasmid containing the RIP 3.1 promoter and the NeuroD gene was bound to cationic microbubbles and infused IV in diabetic baboons. Ultrasound was applied to the baboons' pancreas (see Fig. 15).

5. Oxygen delivery with microbubbles

Compared to liquids, microbubbles hold far higher concentrations of gases, e.g. oxygen [10,11,129–135]. Dodecafluoropentane emulsion (DDFPe), referred to at that time as EchoGen, was studied as an ultrasound contrast agent (USCA) in over 2000 patients [12,13]. It was approved by the European Medicines Agency as an USCA and approvable by the FDA. For use as an USCA it was activated by creating negative pressure in the syringe prior to IV administration [14]. Without hypobaric activation it remained in the condensed, i.e. liquid state, after IV administration. DDFP has boiling point of about 29 °C (less than body temperature) but because of surface tension likely remains condensed unless hypobaric activation is performed prior to administration. DDFPe carries far more oxygen [133] than liquid fluorocarbons that have been tested as oxygen therapeutics, meaning that a low dose of DDFPe is required [134,135]. The liquid fluorocarbons underwent extensive clinical testing

but ultimately failed due to adverse events caused by the high doses necessary to achieve therapeutic oxygen delivery [134,135].

Lundgren et al. showed that DDFPe has therapeutic efficacy in models of hemorrhagic shock using doses of 0.75 cm³ per kg of 2% weight/volume emulsion — a dose that was sufficient to replace the oxygen carrying capacity of the entire blood volume in rats [136]. In pigs a dose of 0.6 cm³ per kg enabled survival of animals subjected to 50% blood loss while all control animals died [137]. NuvOx Pharma (Tucson, AZ) has remanufactured DDFPe nano-emulsion. DDFPe nano-emulsion was tested for oxygen carrying capacity compared to other liquid fluorocarbons (see Fig. 16) [133]. DDFPe carried far more oxygen than the liquid fluorocarbons [133].

5.1. DDFPe as neuroprotectant in stroke

Culp et al., have tested DDFPe as a neuroprotectant in an ischemic stroke model [138,139]. The hypothesis underlying the research is that increasing the oxygen carrying capacity in the blood with DDFPe should improve oxygen supply to ischemic brain tissue in the penumbra to limit the ultimate size of the infarct. Embolic stroke was created in New Zealand white rabbits by injecting microspheres angiographically into the distal internal carotid artery to embolize the middle cerebral artery. The sizes of the brain infarcts were determined histologically. DDFPe was administered at time-points ranging from 1, 3 and 6 h post-stroke. Doses of DDFPe ranging from 0.05 cm³ per kg, to 0.6 cm³ per kg were administered IV every 90 min. Fig. 17 shows results from the 0.1 cm³ per kg dose of DDFPe where the animals were sacrificed 24 h post-infarct. The mean stroke volume in the control animals was significantly different, 3.39% versus 0.51% for the animals treated with DDFPe [138,139].

The above experiments with DDFPe are promising and suggest that this material holds promise as a neuroprotectant. DDFPe might also be used for sonothrombolysis. Borelli of the University of Arkansas
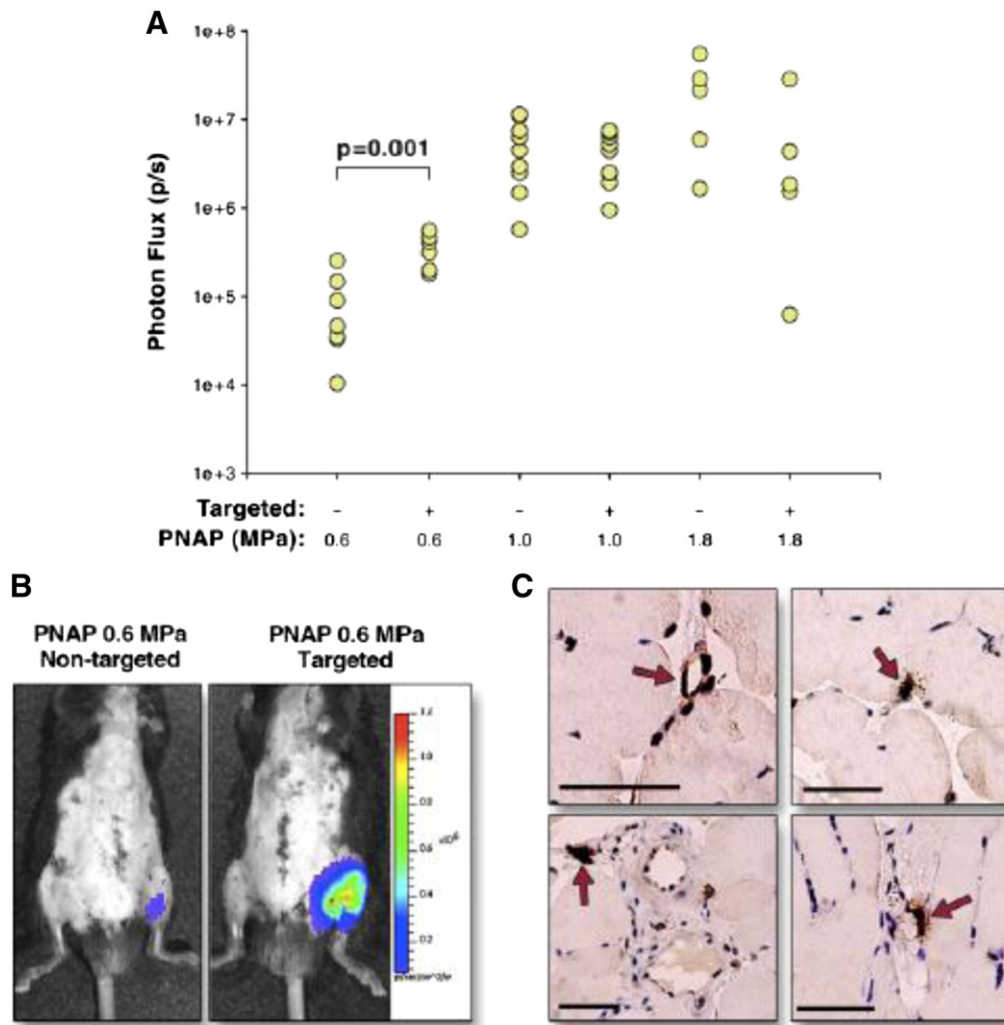
Fig. 13. Targeted transfection of luciferase reporter plasmid. (A) In vivo optical imaging data of luciferase reporter gene transfection 3 days after UTMD, quantified as photon flux at the site of ultrasound exposure 10 min after intraperitoneal injection of luciferin [119]. PNAP—peak negative acoustic pressure. Transfection was significantly lower at 0.6 MPa compared with 1.0 and 1.8 MPa for both agents. (B) Examples illustrating luminescence (color-coded) 3 days after bilateral hind limb ischemia and intravenous injection of either nontargeted or P-selectin-targeted cDNA coupled cationic microbubbles during ultrasound at 0.6 MPa. Ventral surface depilation was performed to reduce light attenuation. (C) Immunohistochemistry for luciferase with peroxidase illustrating transfection (arrows) of venular and capillary endothelium and perivascular cells. Scale bar = 50 μm.
Reference [118], with permission of Elsevier.

(unpublished data) showed that ultrasound application will increase the off-load rate of oxygen from DDFPe. There is potential then to combine oxygen delivery with sonothrombolysis and enhance local oxygen delivery to ischemic cardiac or cerebral tissue with ultrasound. Recently we completed a study testing DDFPe as an oxygen therapeutic for cancer treatment [10]. Administration of DDFPe increased tumor pO_2 by 400% compared to baseline on carbogen breathing [10]. Animals administered DDFPe during radiation had prolonged survival compared with animals treated with radiation without DDFPe [10].

6. Overview — present and future directions

One of the first therapeutic applications of ultrasound for cardiovascular drug delivery has been sonothrombolysis. Ultrasound showed efficacy in treatment of ischemic stroke in association with t-PA without microbubbles. At least one group is continuing efforts in applying ultrasound to treat stroke with t-PA without microbubbles. Microbubbles potentiate sonothrombolysis and have already been used clinically to treat stroke. Hemorrhage is a risk in stroke patients treated with t-PA and high doses of microbubbles in sonothrombolysis may increase risk of hemorrhage; this remains controversial as the increased risk of

hemorrhage in the high microbubble dose cohort could have reflected hemorrhage due to severe stroke with hypertension (factors known to increase the risk of hemorrhage with stroke). Sonothrombolysis has also shown efficacy in treating myocardial infarction both to help restore the epicardial circulation and to help restore circulation in the myocardial microvascular bed, i.e. to decrease the region of "no-reflow." Targeted microbubbles are probably more effective for sonothrombolysis than non-targeted microbubbles, but use of these new bubbles may increase the regulatory challenge associated with entering clinical trials. Targeted microbubbles hold potential for drug and gene deliveries with ultrasound. Studies of gene delivery with ultrasound and microbubbles have advanced from proof of principle studies with reporter genes to studies in disease models showing treatment of important diseases such as myocardial infarction and diabetes with therapeutic genes. Gene delivery studies are currently being performed in large animal models (e.g. diabetes in baboons) to pave the way towards ultimate clinical trials. Microbubbles are highly effective oxygen therapeutics and hold potential as neuroprotectants in stroke and potentially as therapeutic agents to treat myocardial infarction. Ultrasound may enhance local oxygen delivery and thrombolysis using microbubbles not only as cavitation nuclei but also as oxygen therapeutics.
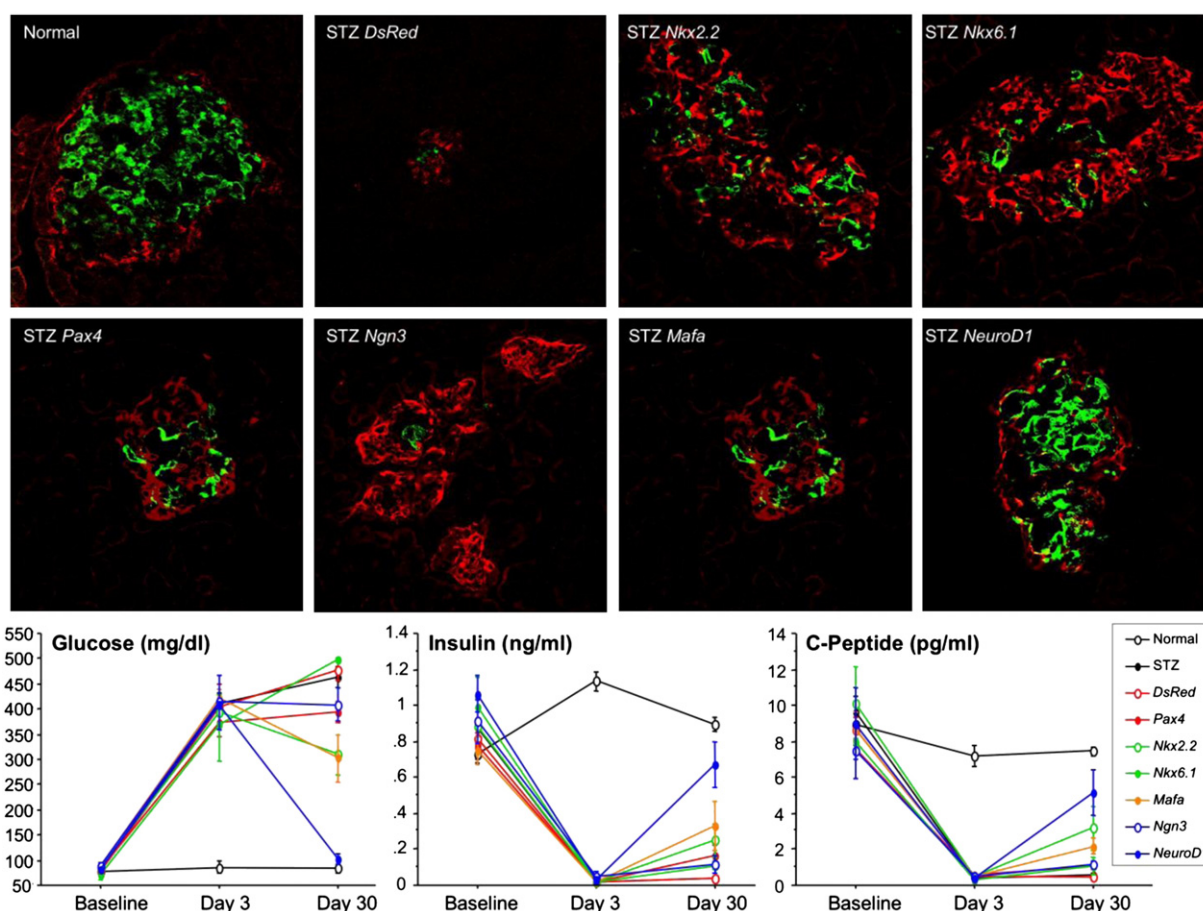
Fig. 14. UTMD gene delivery of RIP 3.1 NeuroD. Gene delivery results in formation of new islets, restoration of normal blood glucose levels, insulin production and C-peptide levels in diabetic rats.
Reference [127], with permission of Nature Publishing Group.

6.1. Regulatory considerations

Microbubbles are regulated as drugs by the FDA under the primary direction of CDER (center for drug evaluation research). Genes and other genetic medicines are generally regulated by the Biologics Division of the FDA. The ultrasound systems are regulated by the Device Division of the FDA. In order for ultrasound-mediated drug delivery systems to become clinically and commercially available, they will have to undergo clinical trials and be approved by the FDA. A new microbubble product candidate will have to undergo extensive pre-clinical safety and pharmacological testing prior to use in clinical trials and will probably have to undergo Phase I safety trials in normal volunteers before it can be used in patients for the therapeutic application in clinical trials. If an existing, i.e. already FDA approved agent, is to be used in clinical trials, it may have to undergo bioeffects testing in animal models according to certified good laboratory practice guidelines, prior to entry into clinical trials in humans. If a combination product is to be developed, e.g. a new microbubble, with a therapeutic gene delivery construct,
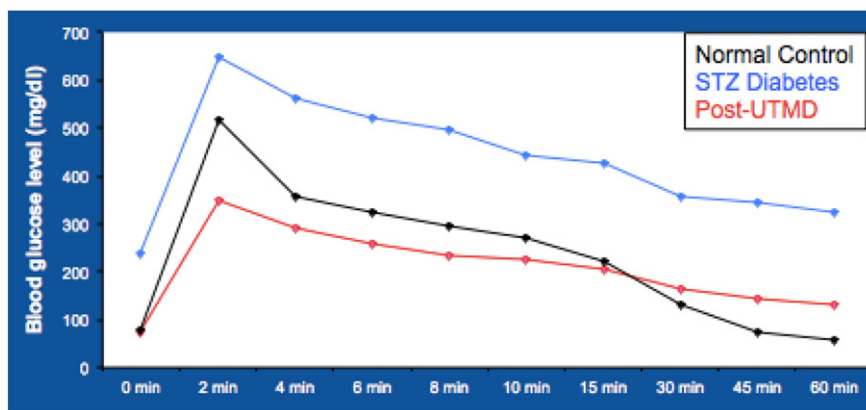

Fig. 15. Glucose tolerance test in 3 different baboons. Glucose tolerance test was performed 21 days post-UTMD. Response in diabetic baboon treated with UTMD gene delivery is similar to normal control. Untreated diabetic animal has higher baseline blood glucose level and persistent hyperglycaemia following glucose challenge.
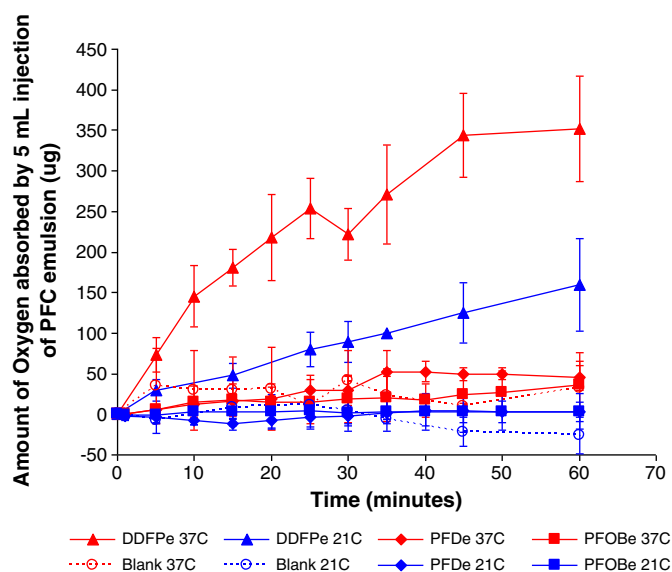
Fig. 16. Comparison of oxygen carrying capacity of DDFPe to liquid fluorocarbons. In vitro study was performed comparing dodecafluoropentane emulsion to perfluorodecalin (PFDe) and perfluorooctylbromide (PFOBe) at 21 and 37 °C. DDFPe carried more oxygen than the higher molecular weight, high boiling point fluorocarbons at either temperature. DDFPe bound even more oxygen at 37 °C consistent with the concept that microbubbles should be even more effective carriers of oxygen [133]. Reproduced with permission of Informa Healthcare.

each component will likely have to undergo extensive pre-clinical testing prior to clinical trials.

6.2. Future directions

Clinical studies are already underway with ultrasound to treat stroke and one company has received the CE-Mark in Europe to sell an ultrasound device to treat stroke. In order to gain approval for this device to treat stroke in the US, however, clinical trials will have to be performed. Clinical studies are underway in Europe testing microbubbles + ultrasound to treat myocardial infarction. The FDA has provided guidance that they will require c-GLP bioeffects studies in animals prior to
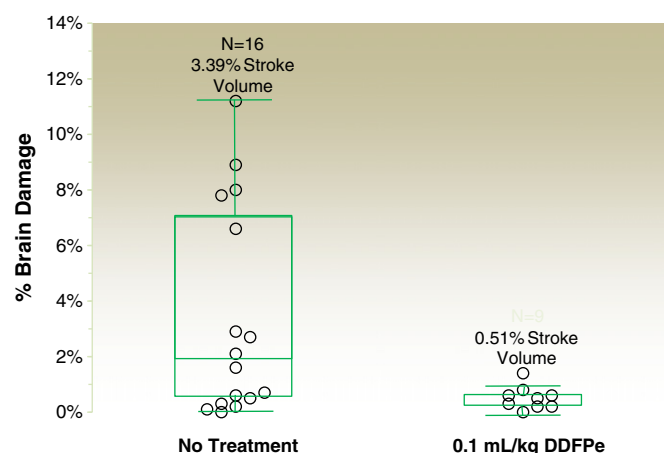

Fig. 17. Effect of DDFPe on stroke volume in rabbits with embolic strokes. Animals were administered DDFPe beginning 1-h following stroke and received repetitive IV bolus doses of 0.1 cm^3 per kg 2% weight/volume emulsion every 90 min following stroke [138,139]. Animals were sacrificed 24 h following stroke and volume of stroke quantitated histologically.

authorizing commencement of clinical trials of sonothrombolysis to treat MI in this country. Targeted microbubbles hold great potential as theranostic agents. One company has commenced clinical trials of a VEG-f targeted microbubble product candidate to evaluate angiogenesis. Hopefully other targeted microbubbles will enter clinical trials. It seems that microbubble and gene delivery technologies are converging, showing sufficient efficacy and benefit that some of these product candidates may enter clinical trials.

6.3. Conclusions

Cardiovascular drug delivery with ultrasound is a promising field with multiple potential applications. Technology in this field holds the potential to minimally or non-invasively afford localized therapy to improve outcomes to treat significant and life-threatening cardiovascular disease. Successful realization of the potential of these technologies will involve drug and device development within a challenging regulatory environment.

References

[1] M.L. Main, M.G. Hibberd, A. Ryan, T.J. Lowe, P. Miller, G. Bhat, Acute mortality in critically ill patients undergoing echocardiography with or without an ultrasound contrast agent, JACC Cardiovasc. Imaging (2013).

[2] R.G. Barr, Off-label use of ultrasound contrast agents for abdominal imaging in the United States, J. Ultrasound Med. 32 (2013) 7–12.

[3] F. Piscaglia, C. Nolsøe, C. Dietrich, D. Cosgrove, O. Gilja, M. Bachmann Nielsen, T. Albrecht, L. Barozzi, M. Bertolotto, O. Catalano, The EFSUMB guidelines and recommendations on the clinical practice of contrast enhanced ultrasound (CEUS): update 2011 on non-hepatic applications, Ultraschall Med. 33 (2012) 33.

[4] M. Claudon, C.F. Dietrich, B.I. Choi, D.O. Cosgrove, M. Kudo, C.P. Nolsøe, F. Piscaglia, S.R. Wilson, R.G. Barr, M.C. Chammas, Guidelines and good clinical practice recommendations for contrast enhanced ultrasound (CEUS) in the liver–update 2012: a WFUMB–EFSUMB initiative in cooperation with representatives of AFSUMB, AIUM, ASUM, FLAUS and ICUS, Ultrasound Med. Biol. (2012).

[5] M. Azmin, C. Harfield, Z. Ahmad, M. Edirisinghe, E. Stride, How do microbubbles and ultrasound interact? Basic physical, dynamic and engineering principles, Curr. Pharm. Des. 18 (2012) 2118–2134.

[6] T. Faez, M. Emmer, K. Kooiman, M. Versluis, A.F. van der Steen, N. de Jong, 20 years of ultrasound contrast agent modeling, IEEE Trans. Ultrason. Ferroelectr. Freq. Control 60 (2013) 7–20.

[7] E. Stride, Physical principles of microbubbles for ultrasound imaging and therapy, Cerebrovasc. Dis. 27 (2009) 1–13.

[8] S.M. Janib, A.S. Moses, J.A. MacKay, Imaging and drug delivery using theranostic nanoparticles, Adv. Drug Deliv. Rev. 62 (2010) 1052–1063.

[9] F. Kiessling, S. Fokong, P. Koczera, W. Lederle, T. Lammers, Ultrasound microbubbles for molecular diagnosis, therapy, and theranostics, J. Nucl. Med. 53 (2012) 345–348.

[10] J.L.H. Johnson, R.A. Leos, A.F. Baker, E.C. Unger, Radiation sensitization for Hs-766T pancreatic tumor xenografts in mice dosed with dodecafluropentane nano emulsion, J. Biomed. Nanotechnol. (2014) (in press).

[11] E.J. Swanson, V. Mohan, J. Kheir, M.A. Borden, Phospholipid-stabilized microbubble foam for injectable oxygen delivery, Langmuir 26 (2010) 15726–15729.

[12] P.A. Grayburn, J.L. Weiss, T.C. Hack, E. Klodas, J.S. Raichlen, M.A. Vannan, A.L. Klein, D.W. Kitzman, S.G. Chrysant, J.L. Cohen, Phase III multicenter trial comparing the efficacy of 2% dodecafluoropentane emulsion (EchoGen) and sonicated 5% human albumin (Albunex) as ultrasound contrast agents in patients with suboptimal echocardiograms, J. Am. Coll. Cardiol. 32 (1998) 230–236.

[13] J.-M. Correas, A.R. Meuter, E. Singlas, D.R. Kessler, D. Worah, S.C. Quay, Human pharmacokinetics of a perfluorocarbon ultrasound contrast agent evaluated with gas chromatography, Ultrasound Med. Biol. 27 (2001) 565–570.

[14] F. Forsberg, R. Roy, D.A. Merton, N.M. Rawool, J.-B. Liu, M. Huang, D. Kessler, B.B. Goldberg, Conventional and hypobaric activation of an ultrasound contrast agent, Ultrasound Med. Biol. 24 (1998) 1143–1150.

[15] http://www.ema.europa.eu/docs/en_GB/document_library?Public_statement/2009/12/WC.

[16] W. Luo, K. Numata, M. Kondo, M. Morimoto, K. Sugimori, K. Hirasawa, A. Nozaki, X. Zhou, K. Tanaka, Sonazoid-enhanced ultrasonography for evaluation of the enhancement patterns of focal liver tumors in the late phase by intermittent imaging with a high mechanical index, J. Ultrasound Med. 28 (2009) 439–448.

[17] G.T. Seidel, K. Meyer, C. Algermissen, A. Broillet, Harmonic imaging of the brain parenchyma using a perfluorobutane-containing ultrasound contrast agent, Ultrasound Med. Biol. 27 (2001) 915–918.

[18] S. Pochon, I. Tardy, P. Bussat, T. Bettinger, J. Brochot, M. von Wronski, L. Passantino, M. Schneider, BR55: a lipopeptide-based VEGFR2-targeted ultrasound contrast agent for molecular imaging of angiogenesis, Invest. Radiol. 45 (2010) 89–95.

[19] http://www.definityimaging.com.

[20] http://optisonimaging.com.

[21] P.C. Sontum, Physicochemical characteristics of Sonazoid™, a new contrast agent for ultrasound imaging, Ultrasound Med. Biol. 34 (2008) 824–833.

[22] M. Schneider, SonoVue, a new ultrasound contrast agent, Eur. Radiol. 9 (1999) S347.

[23] R. Walovitch, H. Bernstein, D. Chickering, J. Straub, Ultrasound contrast agent dosage formulation, in, Google Patents, 2011.

[24] http://www.acusphere.com/product/home.html.

[25] A. Kabalnov, D. Klein, T. Pelura, E. Schutt, J. Weers, Dissolution of multicomponent microbubbles in the bloodstream: 1. Theory, Ultrasound Med. Biol. 24 (1998) 739–749.

[26] M.B. Hampton, M.C. Vissers, J.I. Keenan, C.C. Winterbourn, Oxidant-mediated phosphatidylserine exposure and macrophage uptake of activated neutrophils: possible impairment in chronic granulomatous disease, J. Leukoc. Biol. 71 (2002) 775–781.

[27] T. Faez, D. Goertz, N. De Jong, Characterization of Definity™ ultrasound contrast agent at frequency range of 5–15 MHz, Ultrasound Med. Biol. 37 (2011) 338–342.

[28] D.E. Goertz, N. de Jong, A.F. van der Steen, Attenuation and size distribution measurements of Definity™ and manipulated Definity™ populations, Ultrasound Med. Biol. 33 (2007) 1376–1388.

[29] B.E. Dahneke, Measurement of Suspended Particles by Quasi-Elastic Light Scattering, John Wiley & Sons, 1983.

[30] D.F. Driscoll, F. Etzler, T.A. Barber, J. Nehne, W. Niemann, B.R. Bistrian, Physico-chemical assessments of parenteral lipid emulsions: light obscuration versus laser diffraction, Int. J. Pharm. 219 (2001) 21–37.

[31] D. Driscoll, Examination of selection of light-scattering and light-obscuration acceptance criteria for lipid injectable emulsions, Pharmacopeial Forum, 2004, pp. 2–11.

[32] D.F. Driscoll, Lipid injectable emulsions: pharmacopeial and safety issues, Pharm. Res. 23 (2006) 1959–1969.

[33] US Pharmacopoeidal Forum. Vol 31. No.5. 2005.

[34] C.C. Church, E.L. Carstensen, "Stable" inertial cavitation, Ultrasound Med. Biol. 27 (2001) 1435–1437.

[35] R. Karshafian, P.D. Bevan, R. Williams, S. Samac, P.N. Burns, Sonoporation by ultrasound-activated microbubble contrast agents: effect of acoustic exposure parameters on cell membrane permeability and cell viability, Ultrasound Med. Biol. 35 (2009) 847–860.

[36] C.-D. Ohl, M. Arora, R. Ikink, N. de Jong, M. Versluis, M. Delius, D. Lohse, Sonoporation from jetting cavitation bubbles, Biophys. J. 91 (2006) 4285–4295.

[37] A.F. Lum, M.A. Borden, P.A. Dayton, D.E. Kruse, S.I. Simon, K.W. Ferrara, Ultrasound radiation force enables targeted deposition of model drug carriers loaded on microbubbles, J. Control. Release 111 (2006) 128–134.

[38] P. Dayton, A. Klibanov, G. Brandenburger, K. Ferrara, Acoustic radiation force in vivo: a mechanism to assist targeting of microbubbles, Ultrasound Med. Biol. 25 (1999) 1195–1201.

[39] E. Unger, T. Matsunaga, Gene Delivery with Ultrasound and Microbubbles, INTECH, Non-Viral Gene Therapy, 2011, ISBN 978-953-307-538-9.

[40] E.C. Unger, T.P. McCreery, R.H. Sweitzer, V.E. Caldwell, Y. Wu, Acoustically active lipospheres containing paclitaxel: a new therapeutic ultrasound contrast agent, Invest. Radiol. 33 (1998) 886–892.

[41] Y. Capan, B.H. Woo, S. Gebrekidan, S. Ahmed, P.P. DeLuca, Influence of formulation parameters on the characteristics of poly (D, L-lactide-co-glycolide) microspheres containing poly (L-lysine) complexed plasmid DNA, J. Control. Release 60 (1999) 279–286.

[42] P. Hauff, S. Seemann, R. Reszka, M. Schultze-Mosgau, M. Reinhardt, T. Buzasi, T. Plath, S. Rosewicz, M. Schirner, Evaluation of gas-filled microparticles and sonoporation as gene delivery system: feasibility study in rodent tumor models, Radiology 236 (2005) 572–578.

[43] S.R. Sirsi, S.L. Hernandez, L. Zielinski, H. Blomback, A. Koubaa, M. Synder, S. Homma, J.J. Kandel, D.J. Yamashiro, M.A. Borden, Polyplex-microbubble hybrids for ultrasound-guided plasmid DNA delivery to solid tumors, J. Control. Release 157 (2012) 224–234.

[44] S.R. Sirsi, D. Yamashiro, J. Kandel, M. Borden, Polyplex-microbubbles for ultrasound-mediated gene therapy, Proceedings of Meetings on Acoustics, 2013, p. 075058.

[45] Q. Jin, Z. Wang, F. Yan, Z. Deng, F. Ni, J. Wu, R. Shandas, X. Liu, H. Zheng, A novel cationic microbubble coated with stearic acid-modified polyethylenimine to enhance DNA loading and gene delivery by ultrasound, PLoS One 8 (2013) e76544.

[46] C.W. Burke, E. Alexander, K. Timbie, A.L. Kilbanov, R.J. Price, Ultrasound-activated agents comprised of 5FU-bearing nanoparticles bonded to microbubbles inhibit solid tumor growth and improve survival, Mol. Ther. 22 (2) (2014) 321–328.

[47] J.I. Park, D. Jagadeesan, R. Williams, W. Oakden, S. Chung, G.J. Stanisz, E. Kumacheva, Microbubbles loaded with nanoparticles: a route to multiple imaging modalities, ACS Nano 4 (2010) 6579–6586.

[48] A.L. Klibanov, T.I. Shevchenko, B.I. Raju, R. Seip, C.T. Chin, Ultrasound-triggered release of materials entrapped in microbubble–liposome constructs: a tool for targeted drug delivery, J. Control. Release 148 (2010) 13–17.

[49] A.S. Go, D. Mozaffarian, V.L. Roger, E.J. Benjamin, J.D. Berry, W.B. Borden, D.M. Bravata, S. Dai, E.S. Ford, C.S. Fox, Heart disease and stroke statistics—2013 update a report from the American Heart Association, Circulation 127 (2013) e6–e245.

[50] E.C. Unger, et al., Therapeutic applications of lipid-coated microbubbles, Adv. Drug Deliv. Rev. 56.9 (2004) 1291–1314.

[51] T. Hölscher, et al., In vitro sonothrombolysis with duplex ultrasound: first results using a simplified model, Cerebrovasc. Dis. 28.4 (2009) 365–370.

[52] K. Hagisawa, et al., Thrombus-targeted perfluorocarbon-containing liposomal bubbles for enhancement of ultrasonic thrombolysis: in vitro and in vivo study, J. Thromb. Haemost. 11.8 (2013) 1565–1573.

[53] M. de Saint Victor, et al., Properties, characteristics and applications of microbubbles for sonothrombolysis, Expert opinion on drug delivery, 2014, pp. 1–23.

[54] A. Alonso, et al., In vivo clot lysis of human thrombus with intravenous abciximab immunobubbles and ultrasound, Thromb. Res. 124.1 (2009) 70–74.

[55] C.A. Molina, A.D. Barreto, G. Tsivgoulis, P. Sierzenski, M.D. Malkoff, M. Rubiera, N. Gonzales, R. Mikulik, G. Pate, J. Ostrem, Transcranial ultrasound in clinical sonothrombolysis (TUCSON) trial, Ann. Neurol. 66 (2009) 28–38.

[56] X. Chen, et al., New Insights into Mechanisms of Sonothrombolysis Using Ultra-High-Speed Imaging, Ultrasound Med. Biol. 40.1 (2014) 258–262.

[57] A.V. Alexandrov, C.A. Molina, J.C. Grotta, Z. Garami, S.R. Ford, J. Alvarez-Sabin, J. Montaner, M. Saqqur, A.M. Demchuk, L.A. Moyé, Ultrasound-enhanced systemic thrombolysis for acute ischemic stroke, N. Engl. J. Med. 351 (2004) 2170–2178.

[58] H.P. Adams, R.J. Adams, T. Brott, G.J. del Zoppo, A. Furlan, L.B. Goldstein, R.L. Grubb, R. Higashida, C. Kidwell, T.G. Kwiatkowski, Guidelines for the early management of patients with ischemic stroke a scientific statement from the stroke council of the American stroke association, Stroke 34 (2003) 1056–1083.

[59] H.P. Adams, G. del Zoppo, M.J. Alberts, D.L. Bhatt, L. Brass, A. Furlan, R.L. Grubb, R.T. Higashida, E.C. Jauch, C. Kidwell, Guidelines for the early management of adults with ischemic stroke a guideline from the American Heart Association/American Stroke Association Stroke Council, Clinical Cardiology Council, Cardiovascular Radiology and Intervention Council, and the Atherosclerotic Peripheral Vascular Disease and Quality of Care Outcomes in Research Interdisciplinary Working Groups: the American Academy of Neurology affirms the value of this guideline as an educational tool for neurologists, Circulation 115 (2007) e478–e534.

[60] W. Hacke, M. Kaste, E. Bluhmki, M. Brozman, A. Dávalos, D. Guidetti, V. Larrue, K.R. Lees, Z. Medeghri, T. Machnig, Thrombolysis with alteplase 3 to 4.5 hours after acute ischemic stroke, N. Engl. J. Med. 359 (2008) 1317–1329.

[61] D. Kleindorfer, Y. Xu, C.J. Moomaw, P. Khatri, O. Adeoye, R. Hornung, US geographic distribution of rt-PA utilization by hospital for acute ischemic stroke, Stroke 40 (2009) 3580–3584.

[62] D.Z. Wang, J.A. Rose, D.S. Honings, D.J. Garwacki, J.C. Milbrandt, Treating acute stroke patients with intravenous t-PA the OSF stroke network experience, Stroke 31 (2000) 77–81.

[63] C.A. Molina, M. Ribo, M. Rubiera, J. Montaner, E. Santamarina, R. Delgado-Mederos, J.F. Arenillas, R. Huertas, F. Purroy, P. Delgado, Microbubble administration accelerates clot lysis during continuous 2-MHz ultrasound monitoring in stroke patients treated with intravenous tissue plasminogen activator, Stroke 37 (2006) 425–429.

[64] A.V. Alexandrov, R. Mikulik, M. Ribo, V.K. Sharma, A.Y. Lao, G. Tsivgoulis, R.M. Sugg, A. Barreto, P. Sierzenski, M.D. Malkoff, A pilot randomized clinical safety study of sonothrombolysis augmentation with ultrasound-activated perflutren-lipid micro-spheres for acute ischemic stroke, Stroke 39 (2008) 1464–1469.

[65] S. Meairs, W. Culp, Microbubbles for thrombolysis of acute ischemic stroke, Cerebrovasc. Dis. 27 (2009) 55–65.

[66] A.T. Brown, R. Flores, E. Hamilton, P.K. Roberson, M.J. Borrelli, W.C. Culp, Microbubbles improve sonothrombolysis in vitro and decrease hemorrhage in vivo in a rabbit model, Investig. Radiol. 46 (2011) 202–207.

[67] W.C. Culp, R. Flores, A.T. Brown, J.D. Lowery, P.K. Roberson, L.J. Hennings, S.D. Woods, J.H. Hatton, B.C. Culp, R.D. Skinner, Successful microbubble sonothrombolysis without tissue-type plasminogen activator in a rabbit model of acute ischemic stroke, Stroke 42 (2011) 2280–2285.

[68] R. Flores, L.J. Hennings, J.D. Lowery, A.T. Brown, W.C. Culp, Microbubble augmented ultrasound sonothrombolysis decreases intracranial hemorrhage in a rabbit model of acute ischemic stroke, Invest. Radiol. 46 (2011) 419.

[69] P.A. Lapchak, K. Kikuchi, P. Butte, T. Hölscher, Development of transcranial sonothrombolysis as an alternative stroke therapy: incremental scientific advances toward overcoming substantial barriers, Expert Rev. Med. Devices 10 (2013) 201–213.

[70] M. Daffertshofer, A. Gass, P. Ringleb, M. Sitzer, U. Sliwka, T. Els, O. Sedlaczek, W.J. Koroshetz, M.G. Hennerici, Transcranial low-frequency ultrasound-mediated thrombolysis in brain ischemia increased risk of hemorrhage with combined ultrasound and tissue plasminogen activator: results of a phase II clinical trial, Stroke 36 (2005) 1441–1446.

[71] E. Bor-Seng-Shu, R. De Carvalho Nogueira, E.G. Figueiredo, E.F. Evaristo, A.B. Conforto, M.J. Teixeira, Sonothrombolysis for acute ischemic stroke: a systematic review of randomized controlled trials, Neurosurg. Focus 32 (2012) E5.

[72] J. Eggers, I.R. König, B. Koch, G. Händler, G. Seidel, Sonothrombolysis with transcranial color-coded sonography and recombinant tissue-type plasminogen activator in acute middle cerebral artery main stem occlusion results from a randomized study, Stroke 39 (2008) 1470–1475.

[73] A. Burgess, Y. Huang, A.C. Waspe, M. Ganguly, D.E. Goertz, K. Hynynen, High-intensity focused ultrasound (HIFU) for dissolution of clots in a rabbit model of embolic stroke, PLoS One 7 (2012) e42311.

[74] http://clinicaltrials.gov/show/NCT01098981.

[75] M.J. Davies, A.C. Thomas, Plaque fissuring—the cause of acute myocardial infarction, sudden ischaemic death, and crescendo angina, Br. Heart J. 53 (1985) 363.

[76] H. Suryapranata, A.W. van't Hof, J.C. Hoorntje, M.-J. de Boer, F. Zijlstra, Randomized comparison of coronary stenting with balloon angioplasty in selected patients with acute myocardial infarction, Circulation 97 (1998) 2502–2505.

[77] I. Morishima, T. Sone, S. Mokuno, S. Taga, A. Shimauchi, Y. Oki, J. Kondo, H. Tsuboi, H. Sassa, Clinical significance of no-reflow phenomenon observed on angiography after successful treatment of acute myocardial infarction with percutaneous trans-luminal coronary angioplasty, Am. Heart J. 130 (1995) 239–243.

[78] E.-A. Brujan, Cardiovascular cavitation, Med. Eng. Phys. 31 (2009) 742–751.

[79] S. Kutty, J. Wu, J.M. Hammel, F. Xie, S. Gao, L.K. Drvol, J. Lof, S.J. Radio, S.L. Therrien, D.A. Danford, Microbubble mediated thrombus dissolution with diagnostic ultrasound for the treatment of chronic venous thrombi, PLoS One 7 (2012) e51453.

[80] S. Kutty, F. Xie, S. Gao, L.K. Drvol, S.E. Fletcher, S.J. Radio, D.A. Danford, J.M. Hammel, T.R. Porter, Sonothrombolysis of intra-catheter aged venous thrombi using microbubble enhancement and guided three-dimensional ultrasound pulses, J. Am. Soc. Echocardiogr. 23 (2010) 1001–1006.

[81] F. Xie, J. Lof, T. Matsunaga, R. Zutshi, T.R. Porter, Diagnostic ultrasound combined with glycoprotein IIb/IIIa-targeted microbubbles improves microvascular recovery after acute coronary thrombotic occlusions, Circulation 119 (2009) 1378–1385.

[82] F. Xie, J. Slikkerveer, S. Gao, J. Lof, O. Kamp, E. Unger, S. Radio, T. Matsunaga, T.R. Porter, Coronary and microvascular thrombolysis with guided diagnostic ultrasound and microbubbles in acute ST segment elevation myocardial infarction, J. Am. Soc. Echocardiogr. 24 (2011) 1400–1408.

[83] E. Unger, R. Zutshi, R. Labell, T.R. Porter, J. Lof, F. Xie, K. Ferrara, P. Dayton, S. Bloch, Sonothrombolysis with phospholipid-coated perfluoropropane microbubbles, AIP Conference Proceedings, 2005, p. 58.

[84] S. Datta, C.-C. Coussios, A.Y. Ammi, T.D. Mast, G.M. de Courten-Meyers, C.K. Holland, Ultrasound-enhanced thrombolysis using Definity® as a cavitation nucleation agent, Ultrasound Med. Biol. 34 (2008) 1421–1433.

[85] J. Slikkerveer, S.A. Kleijn, Y. Appelman, T.R. Porter, G. Veen, A.C. van Rossum, O. Kamp, Ultrasound enhanced prehospital thrombolysis using microbubbles infusion in patients with acute ST elevation myocardial infarction: pilot of the Sonolysis study, Ultrasound Med. Biol. 38 (2012) 247–252.

[86] W.M. Júnior, Therapeutic Use of Ultrasound in an Acute and Chronic Coronary Artery Disease, 2013.

[87] S. Moghimi, J. Szebeni, Stealth liposomes and long circulating nanoparticles: critical issues in pharmacokinetics, opsonization and protein-binding properties, Prog. Lipid Res. 42 (2003) 463–478.

[88] A. Klibanov, J. Rychak, W. Yang, S. Alikhani, B. Li, S. Acton, J. Lindner, K. Ley, S. Kaul, Targeted ultrasound contrast agent for molecular imaging of inflammation in high-shear flow, Contrast Media Mol. Imaging 1 (2006) 259–266.

[89] F.S. Villanueva, R.J. Jankowski, S. Klibanov, M.L. Pina, S.M. Alber, S.C. Watkins, G.H. Brandenburger, W.R. Wagner, Microbubbles targeted to intercellular adhesion molecule-1 bind to activated coronary artery endothelial cells, Circulation 98 (1998) 1–5.

[90] B.A. Kaufmann, J.R. Lindner, Molecular imaging with targeted contrast ultrasound, Curr. Opin. Biotechnol. 18 (2007) 11–16.

[91] L. Gerrit, E.J. Sijbrands, J. Folkert, S.B. Feinstein, A.F. van der Steen PhD, M.J. Daemen, A.F. Schinkel, Molecular imaging of inflammation and intraplaque vasa vasorum: a step forward to identification of vulnerable plaques? J. Nucl. Cardiol. 17 (2010) 897–912.

[92] J-M. Hyvelin, et al., Ultrasound Molecular Imaging of Transient Acute Myocardial Ischemia With a Clinically Translatable P-and E-Selectin Targeted Contrast Agent: Correlation With the Expression of Selectins, Invest. Radiol. (2014).

[93] J.R. Lindner, Molecular imaging of myocardial and vascular disorders with ultrasound, JACC Cardiovasc. Imaging 3 (2010) 204–211.

[94] O.J. McCarty, R.B. Conley, W. Shentu, D. Zha, A. Xie, Y. Qi, Y. Zhao, C. Carr, T. Belcik, Molecular imaging of activated von Willebrand factor to detect high-risk atherosclerotic phenotype, JACC Cardiovasc. Imaging 3 (2010) 947–955.

[95] Y. Wu, E.C. Unger, T.P. McCreery, R.H. Sweitzer, D. Shen, G. Wu, M.D. Vielhauer, Binding and lysing of blood clots using MRX-408, Invest. Radiol. 33 (1998) 880–885.

[96] J.R. Lindner, J. Song, F. Xu, A.L. Klibanov, K. Singbartl, K. Ley, S. Kaul, Noninvasive ultrasound imaging of inflammation using microbubbles targeted to activated leukocytes, Circulation 102 (2000) 2745–2750.

[97] T. Utsugi, A.J. Schroit, J. Connor, C.D. Bucana, I.J. Fidler, Elevated expression of phosphatidylserine in the outer membrane leaflet of human tumor cells and recognition by activated human blood monocytes, Cancer Res. 51 (1991) 3062–3066.

[98] G. Koopman, C. Reutelingsperger, G. Kuijten, R. Keehnen, S. Pals, M. Van Oers, Annexin V for flow cytometric detection of phosphatidylserine expression on B cells undergoing apoptosis, Blood 84 (1994) 1415–1420.

[99] E.C. Unger, T.P. McCreery, R.H. Sweitzer, D. Shen, G. Wu, In vitro studies of a new thrombus-specific ultrasound contrast agent, Am. J. Cardiol. 81 (1998) 58G–61G.

[100] E. Unger, P. Metzger III, E. Krupinski, M. Baker, R. Hulett, D. Gabaeff, J. Mills, D. Ihnat, T. McCreery, The use of a thrombus-specific ultrasound contrast agent to detect thrombus in arteriovenous fistulae, Invest. Radiol. 35 (2000) 86.

[101] X. Hua, P. Liu, Y.-H. Gao, K.-B. Tan, L.-N. Zhou, Z. Liu, X. Li, S.-W. Zhou, Y.-J. Gao, Construction of thrombus-targeted microbubbles carrying tissue plasminogen activator and their in vitro thrombolysis efficacy: a primary research, J. Thromb. Thrombolysis 30 (2010) 29–35.

[102] B.P. Davidson, B.A. Kaufmann, J.T. Belcik, A. Xie, Y. Qi, J.R. Lindner, Detection of antecedent myocardial ischemia with multiselectin molecular imaging, J. Am. Coll. Cardiol. 60 (2012) 1690–1697.

[103] E.C. Unger, E. Marinelli, D. El Mehdi, S. Williams, J. Touroo, H. Kaplan, J.L.H. Johnson, E-selectin targeted nanocomposites for imaging uveitis, The 27th Annual Advances in Contrast Ultrasound, September 21, 2012, Chicago, Illinois, 2012.

[104] J.R. Lindner, Molecular imaging of vascular phenotype in cardiovascular disease: new diagnostic opportunities on the horizon, J. Am. Soc. Echocardiogr. 23 (2010) 343–350.

[105] C.E. Thomas, A. Ehrhardt, M.A. Kay, Progress and problems with the use of viral vectors for gene therapy, Nat. Rev. Genet. 4 (2003) 346–358.

[106] S. Hacein-Bey-Abina, C. Von Kalle, M. Schmidt, M. McCormack, N. Wulffraat, P. Leboulch, A. Lim, C. Osborne, R. Pawliuk, E. Morillon, LMO2-associated clonal T cell proliferation in two patients after gene therapy for SCID-X1, Science 302 (2003) 415–419.

[107] E.C. Unger, T.P. McCreery, R.H. Sweitzer, Ultrasound enhances gene expression of liposomal transfection, Invest. Radiol. 32 (1997) 723–727.

[108] E.C. Unger, T.A. Fritz, T. Matsunaga, V. Ramaswami, D. Yellowhair, G. Wu, Therapeutic delivery systems related applications, in, Google Patents, 1996.

[109] R.V. Shohet, S. Chen, Y.-T. Zhou, Z. Wang, R.S. Meidell, R.H. Unger, P.A. Grayburn, Echocardiographic destruction of albumin microbubbles directs gene delivery to the myocardium, Circulation 101 (2000) 2554–2556.

[110] E.C. Unger, T. McCreery, Methods for delivering compounds into a cell, in, Google Patents, 2004.

[111] K. Anwer, G. Kao, B. Proctor, I. Anscombe, V. Florack, R. Earls, E. Wilson, T. McCreery, E. Unger, A. Rolland, Ultrasound enhancement of cationic lipid-mediated gene transfer to primary tumors following systemic administration, Gene Ther. 7 (2000) 1833–1839.

[112] S. Chen, J.-H. Ding, R. Bekeredjian, B.-Z. Yang, R.V. Shohet, S.A. Johnston, H.E. Hohmeier, C.B. Newgard, P.A. Grayburn, Efficient gene delivery to pancreatic islets with ultrasonic microbubble destruction technology, Proc. Natl. Acad. Sci. 103 (2006) 8469–8474.

[113] H. Fujii, S.-H. Li, J. Wu, Y. Miyagi, T.M. Yau, H. Rakowski, K. Egashira, J. Guo, R.D. Weisel, R.-K. Li, Repeated and targeted transfer of angiogenic plasmids into the infarcted rat heart via ultrasound targeted microbubble destruction enhances cardiac repair, Eur. Heart J. 32 (2011) 2075–2084.

[114] J.-I. Suzuki, M. Ogawa, K. Takayama, Y. Taniyama, R. Morishita, Y. Hirata, R. Nagai, M. Isobe, Ultrasound-microbubble-mediated intercellular adhesion molecule-1 small interfering ribonucleic acid transfection attenuates neointimal formation after arterial injury in mice, J. Am. Coll. Cardiol. 55 (2010) 904–913.

[115] N. Nomikou, P. Tiwari, T. Trehan, K. Gulati, A.P. McHale, Studies on neutral, cationic and biotinylated cationic microbubbles in enhancing ultrasound-mediated gene delivery in vitro and in vivo, Acta Biomater. 8 (2012) 1273–1280.

[116] H. Fujii, Z. Sun, S.-H. Li, J. Wu, S. Fazel, R.D. Weisel, H. Rakowski, J. Lindner, R.-K. Li, Ultrasound-targeted gene delivery induces angiogenesis after a myocardial infarction in mice, JACC Cardiovasc. Imaging 2 (2009) 869–879.

[117] E.C. Unger, E. Hersh, M. Vannan, T.O. Matsunaga, T. McCreery, Local drug and gene delivery through microbubbles, Prog. Cardiovasc. Dis. 44 (2001) 45–54.

[118] A. Xie, T. Belcik, Y. Qi, T.K. Morgan, S.A. Champaneri, S. Taylor, B.P. Davidson, Y. Zhao, A.L. Klibanov, M.A. Kuliszewski, Ultrasound-mediated vascular gene transfection by cavitation of endothelial-targeted cationic microbubbles, JACC Cardiovasc. Imaging 5 (2012) 1253–1262.

[119] N.A. Geis, C.R. Mayer, R.D. Kroll, S.E. Hardt, H.A. Katus, R. Bekeredjian, Spatial distribution of ultrasound targeted microbubble destruction increases cardiac transgene expression but not capillary permeability, Ultrasound Med. Biol. 35 (2009) 1119–1126.

[120] Y.-L. Xu, Y.-H. Gao, Z. Liu, K.-B. Tan, X. Hua, Z.-Q. Fang, Y.-L. Wang, Y.-J. Wang, H.-M. Xia, Z.-X. Zhuo, Myocardium-targeted transplantation of mesenchymal stem cells by diagnostic ultrasound-mediated microbubble destruction improves cardiac function in myocardial infarction of New Zealand rabbits, Int. J. Cardiol. 138 (2010) 182–195.

[121] S. Chen, M. Shimoda, J. Chen, P. Grayburn, Stimulation of adult resident cardiac progenitor cells by durable myocardial expression of thymosin beta 4 with ultrasound-targeted microbubble delivery, Gene Ther. 20 (2) (2013) 225–233.

[122] M.A. Kuliszewski, J. Kobulnik, J.R. Lindner, D.J. Stewart, H. Leong-Poi, Vascular gene transfer of SDF-1 promotes endothelial progenitor cell engraftment and enhances angiogenesis in ischemic muscle, Mol. Ther. 19 (2011) 895–902.

[123] A.D. Association, National diabetes fact sheet, Internet: http://www.diabetes.org/uedocuments/NationalDiabetesFactSheetRev.pdf2005 (accessed 20 September 2006).

[124] S.M. Grundy, I.J. Benjamin, G.L. Burke, A. Chait, R.H. Eckel, B.V. Howard, W. Mitch, S.C. Smith Jr., J.R. Sowers, Diabetes and cardiovascular disease: a statement for healthcare professionals from the American Heart Association, Circulation 100 (1999) 1134–1146.

[125] L.H. Kuller, Stroke and diabetes, Diabetes in America, 21995. 449–456.

[126] S. Chen, M. Shimoda, J. Chen, S. Matsumodo, P.A. Grayburn, Transient overexpression of cyclin D2/CDK4/GLP1 genes induces proliferation and differentiation of adult pancreatic progenitors and mediates islet regeneration, Cell Cycle 11 (2012) 695.

[127] S. Chen, M. Shimoda, M.-Y. Wang, J. Ding, H. Noguchi, S. Matsumoto, P.A. Grayburn, Regeneration of pancreatic islets in vivo by ultrasound-targeted gene therapy, Gene Ther. 17 (2010) 1411–1420.

[128] M. Shimoda, S. Chen, H. Noguchi, S. Matsumoto, P. Grayburn, In vivo non-viral gene delivery of human vascular endothelial growth factor improves revascularisation and restoration of euglycaemia after human islet transplantation into mouse liver, Diabetologia 53 (2010) 1669–1679.

[129] H.D. Van Liew, M.E. Burkard, C.E. Lundgren, I.M. Tyssebotn, Method for enhancing transport of gases to tissues, in, Google Patents, 1999.

[130] C.E. Lundgren, I.M. Tyssebotn, H.D. Van Liew, M.E. Burkard, Method for enhancing transport of gases to tissues, in, Google Patents, 2000.

[131] M.E. Burkard, H.D. Van Liew, Oxygen transport to tissue by persistent bubbles: theory and simulations, J. Appl. Physiol. 77 (1994) 2874–2878.

[132] H.D. Van Liew, M.E. Burkard, High oxygen partial pressure in tissue delivered by stabilized microbubbles, Oxygen Transport to Tissue XVIII, Springer, 1997, pp. 395–401.

[133] J.L. Johnson, M.C. Dolezal, A. Kerschen, T.O. Matsunaga, E.C. Unger, In vitro comparison of dodecafluoropentane (DDFP), perfluorodecalin (PFD), and perfluoroctylbromide (PFOB) in the facilitation of oxygen exchange, Artif. Cells Blood Substit. Immobil. Biotechnol. 37 (2009) 156–162.

[134] J.G. Riess, Understanding the fundamentals of perfluorocarbons and perfluorocarbon emulsions relevant to in vivo oxygen delivery, Artif. Cells Blood Substit. Immobil. Biotechnol. 33 (2005) 47–63.

[135] B. Remy, G. Deby-Dupont, M. Lamy, Red blood cell substitutes: fluorocarbon emulsions and haemoglobin solutions, Br. Med. Bull. 55 (1999) 277–298.

[136] C.E. Lundgren, G.W. Bergoe, I.M. Tyssebotn, Intravascular fluorocarbon-stabilized microbubbles protect against fatal anemia in rats, Artif. Cells Blood Substit. Immobil. Biotechnol. 34 (2006) 473–486.

[137] C.E. Lundgren, I.M. Tyssebotn, AWARD NUMBER: W81XWH-07-1-0011 TITLE: Development of a Minimal-Bulk Oxygen Delivery Product to Enhance Survival During Hemorrhagic Shock/Studies Regarding the Use of Perfluorocarbon-Derived Intravascular Microbubbles from Oxygen Transport Final Report to USAMRMC, 2008.

[138] W.C. Culp, S.D. Woods, R.D. Skinner, A.T. Brown, J.D. Lowery, J.L. Johnson, E.C. Unger, L.J. Hennings, M.J. Borrelli, P.K. Roberson, Dodecafluoropentane emulsion decreases infarct volume in a rabbit ischemic stroke model, J. Vasc. Interv. Radiol. 23 (2012) 116–121.

[139] S.D. Woods, R.D. Skinner, A.M. Ricca, A.T. Brown, W.C. Culp, Progress in dodecafluoropentane emulsion as a neuroprotective agent in a rabbit stroke model, Mol. Neurobiol. 48 (2) (2013) 363–367.